COMPUTATIONAL MODELING AND ANALYSIS OF INSULIN-INDUCED EUKARYOTIC TRANSLATION INITIATION

A Thesis

Presented to the Faculty of the Graduate School

of Cornell University

in Partial Fulfillment of the Requirements for the Degree of

Master of Science

by

Joshua Paul Lequieu

August 2011

COMPUTATIONAL MODELING AND ANALYSIS OF INSULIN-INDUCED EUKARYOTIC TRANSLATION INITIATION

Joshua Paul Lequieu, M.S.

Cornell University 2011

Insulin, the primary hormone regulating the level of glucose in the bloodstream, modulates a variety of cellular and enzymatic processes in normal and diseased cells. Insulin signals are processed by a complex network of biochemical interactions which ultimately induce gene expression programs or other processes such as translation initiation. Surprisingly, despite the wealth of literature on insulin signaling, the relative importance of the components linking insulin with translation initiation remains unclear. We addressed this critical question by developing and interrogating a family of mathematical models of insulin induced translation initiation. The insulin network was modeled using mass-action kinetics within an ordinary differential equations (ODEs) framework. Model parameters were estimated, starting from an initial best fit parameter set, using 24 experimental data sets taken from literature. The residual between model simulations and each of the experimental constraints was simultaneously minimized using the multiobjective POETs algorithm. Sensitivity and robustness analysis were used to identify the key regulatory components of the network under different operational conditions. Our analysis suggested that without insulin, a balance between the pro-initiation activity of the GTP-binding protein Rheb and anti-initiation activity of PTEN controlled basal initiation. On the other hand, in the presence of insulin a combination of PI3K and Rheb activity controlled inducible initiation, where PI3K was only critical in the presence

of insulin. Other well known regulatory mechanisms governing insulin action, for example IRS1 negative feedback, modulated the relative importance of PI3K and Rheb, but did not fundamentally change the signal flow.

BIOGRAPHICAL SKETCH

Joshua was born in San Jose, California to Katherine and Charles Lequieu. He grew up in Cupertino, California and graduated from Monta Vista High School in 2006. Joshua received his Bachelors of Science from Cornell in Chemical Engineering in 2010. Outside of his coursework, Joshua has been active in several campus organizations such as Grace Christian Fellowship, the Chesterton House, and Campus on a Hill. Joshua also enjoys playing and listening to music and reading good books by thoughtful (and often dead) writers.

This document is dedicated to my parents, who's care and guidance have helped me become who I am today.

ACKNOWLEDGEMENTS

First and foremost I am thankful to Professor Jeffrey D. Varner for his invaluable role as my advisor throughout this process. My experiences in his lab have shown me the joy of science and have significantly impacted my future career interests and plans. I am also grateful to Anirikh Chakrabarti whose patience and advice can be seen on nearly every page of this document. Anirikh has been a valued colleague and friend whose support has truly made this work possible. Ryan Tasseff, Tom Mansell, Joe Wayman and Joycelyn Chan have also provided helpful thoughts and insights throughout this process. I am grateful to Nicholas Chisholm, Hassei Takahashi and Bo Hu for their friendship and for fostering my interest in academic research. Justin McGeary, Karl Johnson and the other men of the Chesterton House have played an significant role in helping me to think through the role of work in the life of a Christian. Lastly, I am thankful to God who made this world and who gave us minds to explore and understand it.

TABLE OF CONTENTS

LIST OF TABLES

LIST OF FIGURES

CHAPTER 1

INTRODUCTION

1.1 Paths towards systems biology

The unfolding of events in the life cycle of an organism exhibits an admirable regularity and orderliness, unrivaled by anything we meet with in inanimate matter. We find it controlled by a supremely well-ordered group of atoms, which represent only a very small fraction of the sum total in every cell. Moreover, from the view we have formed of the mechanism of mutation we conclude that the dislocation of just a few atoms within the group of 'governing atoms' of the germ cell suffices to bring about a well-defined change in the large-scale hereditary characteristics of the organism. These facts are easily the most interesting that science has revealed in our day.

- Erwin Schrödinger *What is Life?*
(Cambridge University Press, 1944)

When Erwin Schrödinger wrote his famous treatise, *What is Life?*, he was profoundly interested in a seeming paradox observed in biological systems [103]. In chemistry and physics, molecular behavior is fundamentally governed by entropic forces: chaos is favored, order is not. Interestingly, these fields have shown that underlying disorder can in fact result in a population-averaged behavior that is quite orderly. This "order from disorder" paradigm not only follows from a thermodynamic basis but also fits nicely with the seemingly orderliness of day-to-day events (i.e. apples always fall vertically towards the ground). Biological systems on the other hand, are observed to be quite

different. Schrödinger was troubled by the underlying order of biological systems. Whereas the order observed in physics was a result of random events, biology resulted from a "well-ordered group of atoms" who's global behavior was both surprisingly ordered and extraordinarily complex. This "order-from-order" paradigm seemed out of place next to the contrasting "order from disorder" paradigm of the other sciences. Though perhaps years before his time, echoes of Schrödinger's questions continue to be heard even today. How do biological systems fundamentally function? How does a small population of 'governing atoms' lead to biological diversity? What, at its truly fundamental level, is life?

1.1.1 Molecular biology and biotechnology

These questions began to find answers through the rapid growth of molecular biology in the 1940's, 50's and 60's. Discoveries in this time period firmly established molecular biology as a field that could provide unique insights into the function of biological systems. Perhaps the most significant discoveries of this time period involved the discovery of DNA structure and function. In 1944, Oswald Avery identified DNA as the genetic material of bacterial cells [4]. Eight years later, Alfred Hershey and Martha Chase, confirmed this result by showing that a bacteriophage was simply a container that held its genetic material, a material identified as DNA [44]. Later in 1953, Jim Watson and Francis Crick demonstrated the double-helix structure of DNA and the complementary binding of its four different base pairs [128]. The correspondence of DNA sequence to amino acid sequence of proteins was established by studies performed by Vernon Ingram and Crick in 1957. In the years from 1957 to 1960, Francois Jacob

and Jacques Monod identified the regulatory elements of lactose induction in *Escherichia coli* [51]. The results from these studies are now infamously known as the LAC operon.

The 1970s saw the emergence of genetic engineering and biotechnology. Site-specific restriction enzymes, the workhorses of molecular biology [86], were first discovered by Hamilton O. Smith in 1970 [106]. One year later, Danna and Nathans showed that DNA cleaved by restriction enzymes could be separated by size using gel electrophoresis [22]. It was not long after these pioneering studies that recombinant DNA and biotechnology began to emerge [65, 49, 19]. In 1982, the US Food and Drug Administration approved Eli Lily's 'human'-insulin, the first commercially available drug produced by recombinant DNA technology [54]. This time period also witnessed the growth of DNA sequencing technology. In 1977, Sanger *et al.* developed a method for determining the nucleotide sequence of DNA [95]. This process was later improved by Hood and colleagues in 1986 [112] and then automated by Applied Biosystems in 1987. The powerful DNA amplification technique now known as Polymerase Chain Reaction (PCR) was developed by Kary Mullis in 1983 [7].

1.1.2 The birth of 'omics' data sets

Throughout the following decade into the mid 1990s, further automation of biological assays allowed the generation of genome scale 'omics' data sets. In 1995, the entire genome of *Haemophilus influenzae* was sequenced, a significant achievement marking a notable transition in the nature of biological research [29]. In the next year, microarray analysis emerged as a method to asses the rel-

ative abundance of different RNA transcripts within the cell [99, 17]. This time period also witnessed the rise of proteomic data sets, measurements of each protein expressed by the genome [77]. Seemingly overnight, biological research was transformed from a historically data-poor field to one that was data-rich. Biologists discovered that these 'omics' data sets could describe the levels of virtually all biomolecules in cell [55].

The paramount accomplishment of all these 'omics' data sets was the sequencing of the human genome, a decade long process eventually completed in 2001 by Venter *et al.* [124]. Yet despite this triumph of biological research, Venter *et al.* rightfully acknowledge that sequencing the human genome was only the beginning,

> *"The next steps are clear: We must define the complexity that ensues when this relatively modest set of about 30,000 genes is expressed . . . The sequence is only the first level of understanding of the genome. All genes and their control elements must be identified; their functions, in concert as well as in isolation, defined; their sequence variation worldwide described; and the relation between genome variation and specific phenotypic characteristics determined. Now we know what we have to explain."*

As 'omics' changed the landscape of biological research, researchers were faced with the challenge of interpreting these massive data sets. It was no longer sufficient to simply identify the the levels genes, mRNA and proteins in a cell. Researchers began to ask how these many signals were integrated *together* to generate behavior of the whole: how does global behavior form from the function of its individual parts? The stage was set for the emergence of a new field

that sought to understand biology at a global, systems-level scale. The answer was systems biology, a field to whom we now turn.

1.2 Systems Biology

1.2.1 An overview of systems biology

The goal of systems biology is to develop an understanding of biology at the systems level. In contrast to the reductionist approaches of molecular biology, systems biology adopts an integrative paradigm that seek to understand how large numbers genes and proteins interact together. Hiroaki Kitano, the self proclaimed father of systems biology writes,

> *"Identifying all the genes and proteins in an organism is like listing all the parts of an airplane. While such a list provides a catalog of the individual components, by itself it is not sufficient to understand the complexity underlying the engineered object. We need to know how these parts are assembled to form the structure of the airplane."* [59]

This is the aim of systems biology: to move beyond a simple parts list to an understanding of how each part integrates together to form behavior of the whole. In other words, systems biology offers an opportunity to understand how phenotype results from genotype. In the words of Alan Aderem, co-founder of the Institute of Systems Biology, "Systems biology is a comprehensive quantitative analysis of the manner in which all the components of a biological system interact functionally over time" [1]. Marc Krischner, the chair of the Department of

Systems Biology at Harvard, writes, "systems biology is the study of the behavior of complex biological organization and processes in terms of the molecular constituents" [57].

In order to gain insight into global systems behavior, both experimental and computational approaches are necessary. Generally, the focus of experimental systems biology is to improve high-throughput genomic and proteomic platforms. This involves developing faster, cheaper and more accurate assays that can give quantitative information about the dynamic state of a biological system [46]. Experimental approaches also aim to clarify the mechanisms and pathways of cellular signaling and gene regulatory logic [59]. Computational approaches generally fall in two main branches, knowledge discovery (or data-mining) and simulation-based analysis [58]. In knowledge discovery, the huge 'omics' data sets are interrogated using computational techniques in order to unearth systems behavior (i.e. inference of gene regulatory networks from mRNA expression profiles). Simulation-based analysis are used to explore systems properties that elude experimental observation. Simulation-based analysis is used to generate hypothesis that can be validated by further experimental studies [58]. In systems biology, both experimental and computational techniques are necessary. Systems biology would cease to function effectively if either of these approaches were divorced from the other.

1.2.2 Systems biology and its successes

In the past several years, systems biology has seen many successes. The scope of 'omics' data sets have expanded dramatically beyond the genome, transcrip-

tome and proteome. New high-throughput methods have been developed to determine both DNA-protein [11, 56, 40] and protein-protein interaction data [20, 14, 111]. Computational approaches have been developed to use this interaction data to infer regulatory [5] and protein-protein interaction networks [52, 84]. Other computational approaches have been used to decompose these networks into modules to identify organizational principles and infer regions of network activity [130, 115]. 'Omics' data has also been used to develop genome scale models of an entire cell. These genome scale models have shown utility at identifying systems properties and guiding experimental design [80, 83]. Systems biology has also shown usefulness in developing improved screens for drug discovery [13, 12].

Another important area of research in systems biology is the development of mechanistic models of biological systems. These models have clarified complex dynamic behavior of signaling events like the MAPK cascade and apoptosis [102, 97, 32]. Mechanistic models can also be used to understand network robustness and fragility. Robustness is defined by the ability of a network to maintain performance in the face of perturbations and uncertainty [110]. Though robustness has been known for years in control engineering [89], recent work has identified biological signaling networks as robust [6, 2]. Further, Carlson *et al.* have shown that networks can be robust to some perturbations while fragile to others [15]. Computational methods have been shown to identify regions robustness and fragility within signaling networks [109] and can be used to identify the important interactions in signaling networks. The insight gained by these models can help researchers to develop better hypothesis and to perform more insightful experiments.

CHAPTER 2

MECHANISTIC MODEL OF INSULIN-MEDIATED EUKARYOTIC TRANSLATION INITIATION

2.1 Introduction

Insulin, the primary hormone regulating the level of glucose in the bloodstream, modulates a variety of cellular and enzymatic processes in normal and diseased cells [133, 73, 21, 88, 101, 131, 26]. The modulation of cellular function by insulin and insulin-like growth factors I/II (IGF-I/II) is a highly complex process, involving negative feedback and signal integration [78, 28, 116, 92, 91, 85, 67]. Insulin and IGF-I/II interact with insulin receptors (IR), and type I/II IGF receptors (IGF-IR/IIR) in addition to other hybrid transmembrane receptors [116]. These interactions ultimately induce gene expression programs or other processes such as translation initiation. Translation rates of many cell-cycle and survival proteins are modulated by growth factor, hormone and other mitogenic signals [8]. Insulin induces the activation of class I Phosphoinositide 3-kinases (PI3Ks), which in turn activate the serine/threonine protein kinase Akt and the mammalian target of rapamycin (mTOR). The PI3K/Akt/mTOR signaling axis is important to a variety of cellular programs, including apoptosis [129] and translation initiation. Activation of the PI3K/Akt/mTOR axis ultimately results in the phosphorylation of eukaryotic translation initiation factor 4E-binding protein (4E-BPx) family members [35]. Phosphorylation of 4E-BPx causes the release the eukaryotic translation initiation factor 4E (eIF4E), which is critical to directing ribosomes to the 7-methyl-guanosine cap structure of eukaryotic mRNAs. Previously, the availability of eIF4E has been shown to be rate

limiting for translation initiation in many eukaryotic cell-lines [132, 8]. Given its central role in cell biology, evolutionarily optimized infrastructure like translation might be expected to be robust or highly redundant. Surprisingly, deregulated translation, especially involving growth-factor or insulin induced initiation mechanisms, has been implicated in a spectrum of cancers [9].

Despite the wealth of literature on insulin signaling, the relative importance of the components linking insulin with translation initiation remains unclear. Many investigators have explored this question using both experimental and computational tools. Taniguchi *et al.* proposed three criterion to identify the critical nodes of insulin signaling: network divergence, degree of regulation and potential crosstalk [116]. Using these criteria, they identified insulin-receptor (IR), PI3K and Akt as the *critical nodes* of insulin action. Our understanding of the insulin signaling interactome has also continued to evolve. For example, Caron *et al.* recently published a comprehensive map of the mTOR signaling network, including a detailed portrait of insulin-induced mTOR activation and its downstream role in translation initiation [16]. Several insightful mathematical models of insulin-signaling have also been published [27, 23, 10, 47]. While these models vary in their focus and biological scope, none has exclusively focused on how insulin stimulation induces translation initiation. This particular question was addressed by Nayak *et al.*, who analyzed a family of detailed mathematical models of growth-factor and insulin-induced translation initiation [75]. The Nayak *et al.* study suggested that Akt/mTOR were structurally fragile, and likely the key elements integrating growth factor signaling with translation initiation. Thus, the Nayak study *et al.* at least partially supported the Taniguchi *et al.* hypothesis. However, the Nayak *et al.* model neglected several key features of insulin processing, e.g., negative feedback of IR resulting

from mTOR activity.

The objective of this study was to rank-order the importance of components of insulin-induced translation initiation using computational tools. Toward this objective, we developed and analyzed an ensemble of mechanistic mathematical models of insulin induced translation initiation that was a significant extension of our previous work [75]. First, we expanded the original model connectivity to include a detailed description of the regulation and activity of insulin, insulin-like growth factor and PDGF receptor family members (including negative feedback). Second, we refined the description of the phosphorylation state of Akt and its downstream role in the activation of the mTORC1 and mTORC2 complexes. Lastly, we used new model estimation and interrogation techniques to generate and analyze an uncorrelated population of initiation models that were simultaneously consistent with 24 qualitative and quantitative data sets. Interrogation of this model population, using sensitivity and knockdown analysis, identified an insulin-dependent switch that controlled translation initiation. Without insulin, a balance between the pro-initiation activity of the GTP-binding protein Rheb and anti-initiation activity of PTEN controlled basal initiation. Rheb knockdown simulations confirmed decreased initiation in the majority of the model population. Surprisingly, we also identified a model subpopulation in which deletion of Rheb or mTORC2 components increased initiation. In these cases, removal of Rheb or mTORC2 components relieved a rate-limiting bottleneck e.g., constrained levels of GTP, leading to increased initiation. On the other hand, in the absence of insulin, translation initiation increased for all models in the population following a PTEN deletion. In the presence of insulin, Rheb and PTEN were no longer the dominant arbiters of initiation; a combination of PI3K and Rheb activity controlled inducible initiation, where PI3K was only crit-

ical in the presence of insulin. PI3K deletion in the presence of insulin removed the ability of the network to process insulin signals, but did not remove initiation altogether. PI3K deletion reduced initiation to approximately 60% of its maximum level. Interestingly, the relative contribution of PI3K versus Rheb to the overall initiation level could be tuned by controlling the level of IRS1 feedback. In the absence of feedback, PI3K was more important than Rheb to signal propagation, while the opposite was true in the presence of feedback. Taken together, our modeling study supported the Taniguchi *et al.* hypothesis that PI3K was a critical node in the insulin-induced initiation network. However, we also found that the role of PI3K was nuanced; PI3K in combination with Rheb-GTP controlled initiation in the presence of insulin, while the combination of PTEN and Rheb controlled the rate of basal initiation.

2.2 Results

2.2.1 Translation initiation model connectivity.

The translation initiation model consisted of 250 protein or mRNA species interconnected by 573 interactions (Fig. 2.1). The model described the integration of insulin and growth-factor signaling with 5'-cap recognition and 80S assembly. While other translation initiation mechanisms exist in eukaryotes, here we focused on cap-mediated translation as the dominant translation mechanism [71]. The model interactome was taken from literature (available as an SBML file in the supplemental materials); the connectivity of insulin- and growth-factor induced translation initiation has been extensively studied [67, 50]. The model

interactome was not specific to a single cell-line. Rather, it was a canonical representation of the pathways involved in insulin and growth-factor induced initiation. Binding of insulin or IGF-I/II with IR or IGF-I/IIR promotes the autophosphorylation of the cytosolic domains of these receptors at tyrosine residues. Receptor autophosphorylation promotes the formation of adaptor complexes, which are anchored in place by insulin receptor substrate (IRSx) family members; IRSx are required for the assembly of adaptor complexes involving the Shc, SoS, Grb2 and Ras proteins [105, 104, 87]. In the model we considered only the IRS-1 protein, and neglected other IRSx family members. Adaptor complex formation ultimately culminates in the activation of the catalytic subunit of PI3K. Among their many roles, PI3Ks catalyze the phosphorylation of the phospholipid PIP2 to form PIP3 [131]. PIP3 is critical to the localization of 3-phosphoinositide-dependent kinase 1 (PDK1) to the membrane, where it phosphorylates the master kinase Akt at Thr308 [72]. Akt is further phosphorylated at Ser473 by the rictor-mammalian target of rapamycin (mTORC2) protein [96]. Once phosphorylated, Akt promotes translation initiation by directly or indirectly activating the mTORC1 protein [133]. Akt directly activates mTORC1 through a novel binding partner known as PRAS40 [94, 38]. However, mTORC1 can also be activated by the GTP bound form of the Ras homologue enriched in brain (Rheb) protein. In the absence of insulin, Rheb is regulated by the tuberous sclerosis complex tumor-suppressor protein TSC1/2, which has GTPase activating protein (GAP) activity. Akt directly phosphorylates TSC1/2 which inhibits its GAP activity and allows Rheb-mediated activation of mTORC1 [48, 70]. Activated mTORC1 plays two key roles in translation initiation; first, it activates ribosomal protein S6 kinase beta-1 (S6K1) and second it phosphorylates eukaryotic translation initiation factor 4E-binding protein (4E-BPx) family members

[41]. In this study we included only 4E-BP1 and modeled a single deactivating phosphorylation site. Phosphorylated 4E-BP1 releases eIF4E, which along with other initiation factors, is critical to directing ribosomes to the 7-methylguanosine cap structure of eukaryotic mRNAs [50].

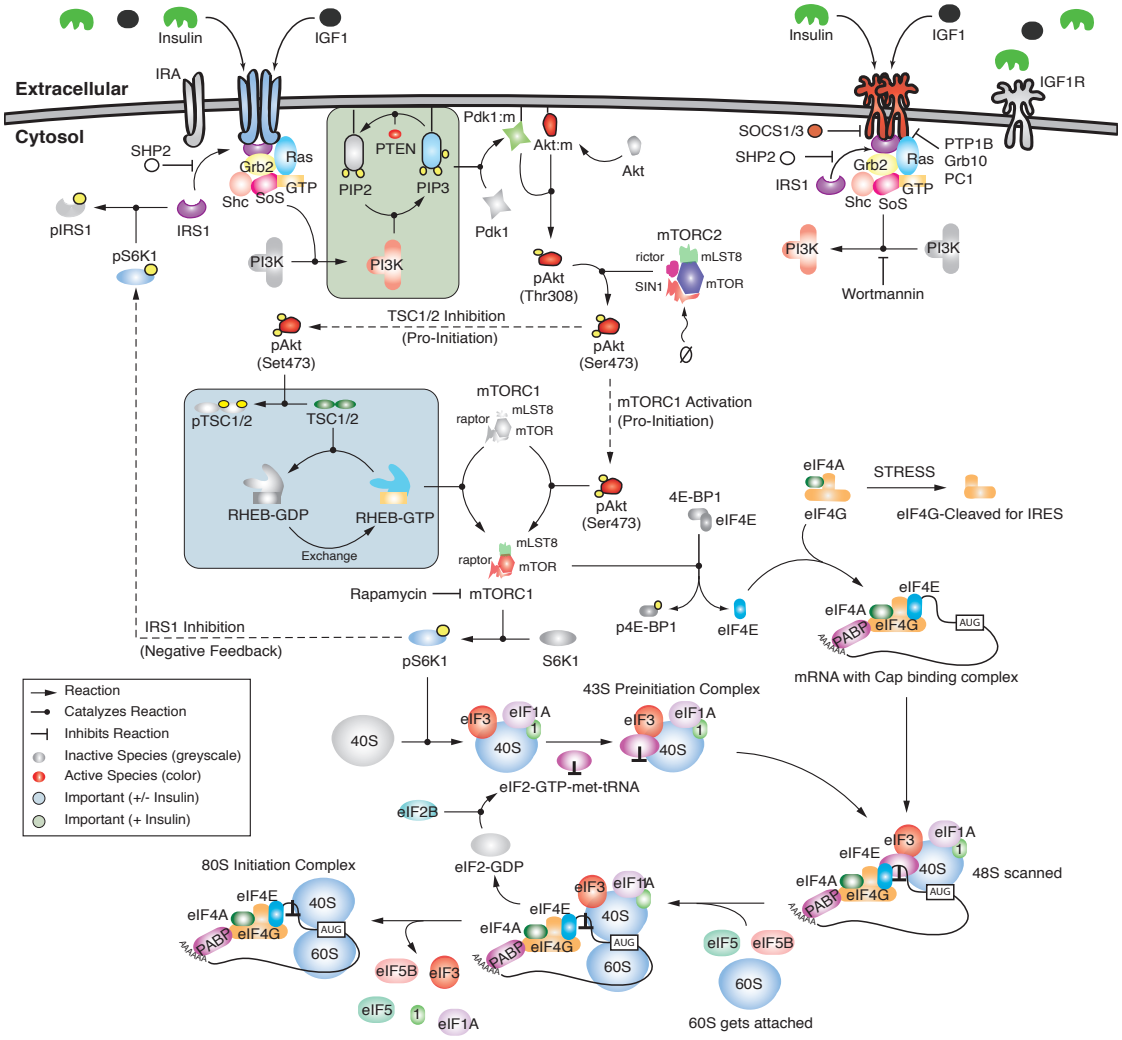

Figure 2.1: Schematic of signaling network. Growth factors result in receptor dimerization and formation of adaptor complexes which activate PI3K. PI3K signals through PIP2/3 to activate Akt. Activated Akt activates mTORC1 either directly or by phosphorylating TSC1/2, an inhibitor of Rheb. Activated mTORC1 can phosphorylate 4EBP1 and activate S6K1, two necessary checkpoints for translation initiation. mTORC1 can also phosphorylate IRS1, a form of negative feedback which inhibits formation of the adaptor complex and attenuates insulin-mediated signaling. See Table A.1 for full species names.

There are many mechanisms which attenuate insulin and growth-factor induced translation initiation. First, several proteins control insulin signal propagation by disrupting adaptor complex formation. For example, we included in the model tyrosine phosphatases and competitive inhibitors such as PTP1B, SHP2, Grb10 and SOCS1/3 which interfere with adaptor complex formation and activity [116, 25, 74, 120]. Second, several mechanisms control PIP3 formation, PDK1 recruitment and Akt phosphorylation [116]. In the model we included the phosphatase and tensin homolog (PTEN) protein, which is known to dephosphorylate PIP3 [113], and SH2 (Src homology 2)-containing inositol phosphatase-1 (SHIP1) which hydrolyses the 5'-phosphates from PIP3 [63]. Lastly, S6K1 can phosphorylate IRS-1 at Ser318, thus inhibiting its function [37]. This S6K1/IRS-1 feedback mechanism has been shown to be important in insulin resistance and cancer [67, 122, 121, 24].

2.2.2 Estimating an ensemble of translation initiation models using POETs.

Translation initiation was modeled using mass action kinetics within an ordinary differential equation (ODE) framework. ODEs and mass-action kinetics are common methods of modeling biological pathways [32, 102, 18, 42]. However, ODEs require a large number of unknown model parameters. For the initiation model, these parameters were not uniquely identifiable (data not shown). Instead, we estimated an experimentally constrained population of parameters using multiobjective optimization. Model parameters were estimated, starting from an initial best fit parameter set, using 24 experimental data sets taken from

literature (Table 2.1). Both *in-vitro* and *in-vivo*, dynamic and steady state measurements from multiple cell-lines were used for model training. The residual between model simulations and each of the experimental constraints was simultaneously minimized using the multiobjective POETs algorithm [107]. In total, 823 unknown parameters (573 kinetic parameters and 250 initial conditions) were estimated using the POETs. We used a leave-three-out cross-validation strategy to independently estimate the prediction and training error during parameter estimation (Table 2.1). Three of the twenty-four objectives were reserved for validation, while the remaining 21 were used for model training. Thus, we estimated eight model families, each of which was trained and validated on different experimental data. Additionally, a random parameter set control was run to check the training/prediction fitness above random (Table 2.1). The random control was generated from 100 random parameter sets with parameter values independent of the nominal set. For 21 of the 24 objectives, the model *prediction* error was statistically significantly better than the random control (t-test, p-value = 0.05). Two remaining objectives (O4 and O12) trained on species heavily constrained by other objective functions e.g., pAkt(Thr308 and Ser473). POETs generated 18,886 probable models with Pareto rank ≤ 4. The performance of 5,818 rank-zero models against selected training objectives is shown in Fig. 2.2. The majority of objective function pairs were uncorrelated e.g., O4×O13 or O12×O13. Uncorrelated objectives suggested the ensemble independently described each of the training objectives. Other objective function pairs were directly proportional e.g., O3×O11 or O9×O15. This trend suggested complementary training data. Interestingly, certain objectives were inversely proportional e.g., O12×O14. For these pairs, the model was unable to simultaneously fit both training data sets. Surprisingly, these objectives were iden-

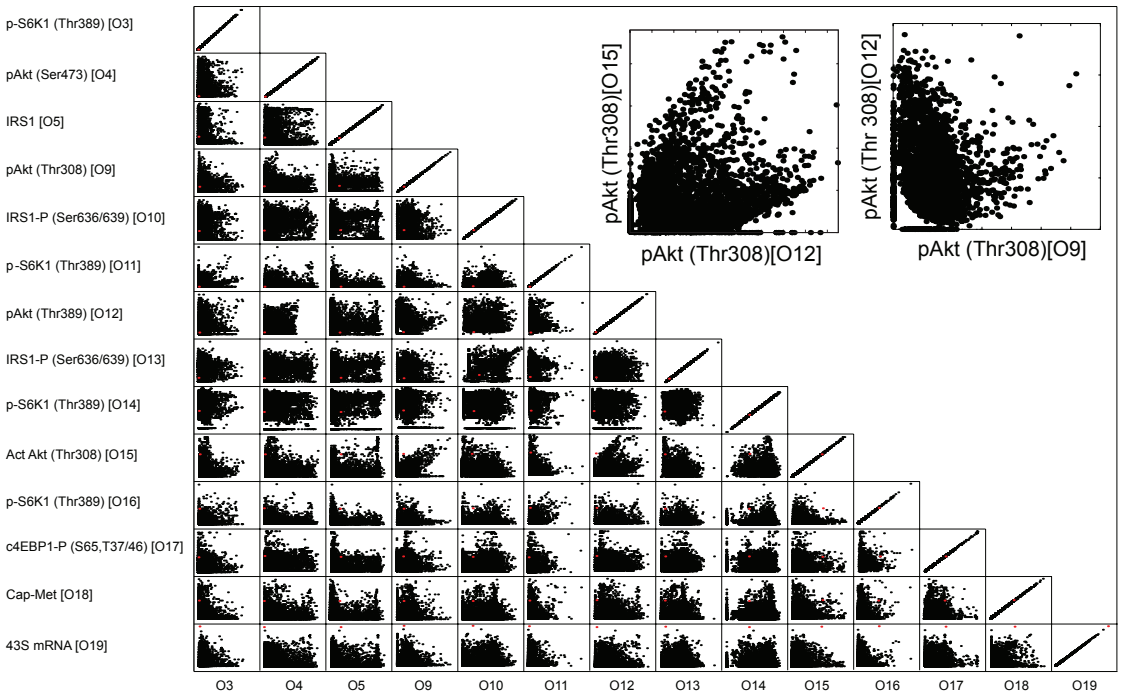

Figure 2.2: Pareto Optimization. The Scaled Simulation Error (SSE) for rank-zero sets identified by POETs were plotted for each objective function pair. 14 of the total 24 sets used for model training are shown. If a objective function was chosen by cross-validation for prediction, the SSE of that objective function was set to zero and disregarded when ranking other sets. Red point indicates error of nominal set.

tical protein measurements in similar experiments pAkt(Thr308) O9×O12 and pS6K1(Thr389) O3×O14, taken either in different cell-lines or different labs. This suggested conflicts in the data e.g., cell-line variation or differences in specific laboratory protocols, rather than structural inaccuracies in the model, were responsible for the inverse relationship.

Table 2.1: Objective function list along with species, cell-type, cellular compartment, nominal error, training error, prediction error, random error with a randomly generated parameter set and the corresponding literature reference.

O#	species	cell type	nominal	training	prediction	random	source
O1	PI3K Activity	3T3-L1 cells	0.01	0.01 ± 0.00	0.01 ± 0.00	0.67 ± 0.20	[62]
O2	PIP3	3T3-L1 cells	0.00	0.00 ± 0.00	0.00 ± 0.00	0.84 ± 0.08	[62]
O3	p-S6K1(T389)	3T3-L1 cells	0.39	0.17 ± 0.15	0.27 ± 0.24	1.55 ± 0.49	[38]
O4	AKT act (S473)	3T3-L1 cells	0.38	0.30 ± 0.23	0.53 ± 0.29	0.50 ± 0.38	[38]
O5	IRS1	3T3-L1 cells	0.43	0.47 ± 0.62	1.37 ± 0.71	0.56 ± 0.58	[38]
O6	AKT act (S473)	393T cells	0.06	0.28 ± 0.32	0.43 ± 0.35	1.10 ± 0.31	[38]
O7	AKT act (S473)	C2C12 myotubes	0.05	0.12 ± 0.13	0.12 ± 0.13	0.69 ± 0.11	[61]
O8	p-S6K1 (T421/S424)	C2C12 myotubes	0.20	0.18 ± 0.07	0.20 ± 0.10	0.47 ± 0.22	[61]
O9	Act AKT (T308)	HUVEC cells	1.21	0.78 ± 0.38	0.94 ± 0.36	1.20 ± 0.79	[43]
O10	IRS1-P (S636/639)	L6 Myotubes	1.34	1.17 ± 0.37	1.13 ± 0.35	1.28 ± 0.38	[119]
O11	p-S6K1 (T389)	L6 Myotubes	0.98	0.27 ± 0.33	0.55 ± 0.64	2.95 ± 0.51	[119]
O12	Act Akt (T308)	L6 Myotubes	0.93	0.62 ± 0.36	0.71 ± 0.34	0.84 ± 0.48	[119]
O13	IRS1-P (S636/639)	L6 Myotubes	1.24	1.07 ± 0.38	1.29 ± 0.31	1.35 ± 0.36	[119]
O14	p-S6K1 (T389)	L6 Myotubes	2.36	2.02 ± 0.43	2.26 ± 0.24	1.95 ± 0.38	[119]
O15	Act Akt (T308)	L6 Myotubes	0.97	0.39 ± 0.35	0.48 ± 0.33	0.87 ± 0.82	[119]
O16	p-S6K1 (T389)	RhoE 3T3 cells	1.33	0.28 ± 0.33	0.21 ± 0.25	2.94 ± 0.54	[125]
O17	c4EBP-P (S65, T37/46)	RhoE 3T3 cells	0.37	0.57 ± 0.33	0.85 ± 0.38	1.76 ± 0.43	[125]
O18	Cap-Met-Puro	rabbit reticulocytes	0.46	0.42 ± 0.46	0.86 ± 0.73	1.24 ± 0.71	[66]
O19	43S-mRNA	rabbit reticulocytes	0.19	0.37 ± 0.39	0.57 ± 0.47	1.14 ± 0.64	[66]
O20	AKT act (S473)	A14 NIH 3T3 cells	1.12	0.98 ± 0.23	0.99 ± 0.23	1.16 ± 0.15	[34]
O21	p-S6K1 (T389)	A14 NIH 3T3 cells	1.20	0.57 ± 0.29	0.57 ± 0.23	0.69 ± 0.21	[34]
O22	Rheb	HeLa cells	0.00	0.15 ± 0.83	0.10 ± 0.71	1.99 ± 0.09	[34]
O23	p-S6K1 (T389)	HeLa cells	0.13	0.14 ± 0.11	0.24 ± 0.23	0.77 ± 0.58	[34]
O24	c4EBP1-P (T70)	HEK293 cells	0.25	0.34 ± 0.26	0.62 ± 0.41	0.90 ± 0.22	[34]

The ensemble of translation models recapitulated diverse training data across multiple cell-lines (Table 2.1). The key indicators of translation initiation in eukaryotes are the phosphorylation of S6K1 and 4E-BP1 [41]. Both Tzatos *et al.* and Villalonga *et al.* performed insightful studies exploring the dynamics of S6K1 and 4E-BP1 phosphorylation in L6 Myotubes and RhoE 3T3 cells [119, 125]. The ensemble recapitulated these observations ($\epsilon_{train} = 0.27 \pm 0.33$, $\epsilon_{rand} = 2.95 \pm 0.51$; $\epsilon_{train} = 0.57 \pm 0.33$, $\epsilon_{rand} = 1.76 \pm 0.43$) (Fig. 2.3A and 2.3B). Further, the ensemble of models was able to respond accurately to growth factors insulin and FBS (Fig. 2.3A and 2.3B). The model was also able to recapitulate IGF1 induced responses ($\epsilon_{train} = 0.12 \pm 0.13$, $\epsilon_{rand} = 0.69 \pm 0.11$; $\epsilon_{train} = 0.18 \pm 0.07$, $\epsilon_{rand} = 0.69 \pm 0.11$) (Fig. 2.3E and 2.3F). Lorsh *et al.* studied the dynamics of ribosomal assembly in rabbit reticulocytes and identified key kinetic parameters in both 43S and 80S assembly [66]. Most importantly, Lorsh *et al.* discovered that the formation of the tertiary complex (eIF2:GTP:Met-tRNA) was the rate limiting step in 80S* formation. Our model captured the 80S* dynamics, including this crucial lag phase in the first two minutes of stimulation ($\epsilon_{train} = 0.42 \pm 0.46$, $\epsilon_{rand} = 1.24 \pm 0.71$) (Fig. 2.3C). The effect of inhibitors was used to train the network for different modes of operation. In the absence of insulin, PI3K is not activated and pAkt (Ser473) levels remain very low (Fig 2.3D, lane 1). Upon stimulation with insulin, PI3K activation results in increased levels of pAkt (Ser473) (Fig 2.3D, lane 2). Wortmanin is a PI3K inhibitor that prevents signaling downstream of PI3K to Akt. Thus, in the presence of insulin and wortmanin, pAkt (Set473) levels significantly decrease (Fig 2.3D, lane 3). While our model qualitatively captures this decrease, the model predicts levels of pAkt (Ser473) that are higher than those observed experimentally. Though our model was not explicitly constrained on levels of mTORC1/2, significant constraints were placed

on the species immediately upstream and downstream of mTORC1/2, namely pAkt (Ser473) and S6K1. Experimental data using rapamycin, a common inhibitor of mTORC1, was also used to constrain mTORC1 mediated signaling. In the absence of insulin, levels of pAkt(Ser473) and S6K1(Thr421/Ser424) are very low (Fig 2.3E/F, lanes 1). Addition of insulin results in increased activity of these species. Upon rapamycin addition, mTORC1 is impaired and levels of phosphorylated S6K1 decrease (Fig. 2.3E, lane 3). However, because of its position upstream of mTORC1, pAkt(Set473) levels are unimpaired (Fig. 2.3E, lane 3).

The predictive ability of the model was tested by comparing model simulations with *in-vivo* and *in-vitro* data sets not used for training (Table 2.2). For all five prediction data sets, the model demonstrated errors statistically significantly better that the random control (t-test, p-value = 0.05). Data from Lorsh *et al.* was used to validate the dynamics of intermediate ribosomal complexes [66]. The level of 43S mRNA was quantified using both GTP and a non-degradable GTP-like homologue GMP-PNP (Fig. 2.4A). Data involving GMP-PNP was used for training while data involving GTP was used only for validation. The model was able to accurately predict this data ($\epsilon_{pred} = 0.52 \pm 0.40$, $\epsilon_{rand} = 0.82 \pm 0.51$). Garami *et al.* explored the insulin-mediated activation of Rheb and the role of its inhibitors TSC1/2 [34]. In another part of their study, Garami *et al.* investigated the effect of wortmanin and rapamycin on the ratio of GTP to GDP bound Rheb [34]. While our model captured the qualitative trends, we over-predicted the percentage of GTP bound Rheb ($\epsilon_{pred} = 0.22 \pm 0.11$, $\epsilon_{rand} = 0.42 \pm 0.01$) (Fig. 2.4B). The model also failed to predict the sustained levels of Rheb-GTP in the presence of rapamycin . This suggested that the sustained levels of pAkt(Ser473) (observed in Figure 2.3E) did not correlate with

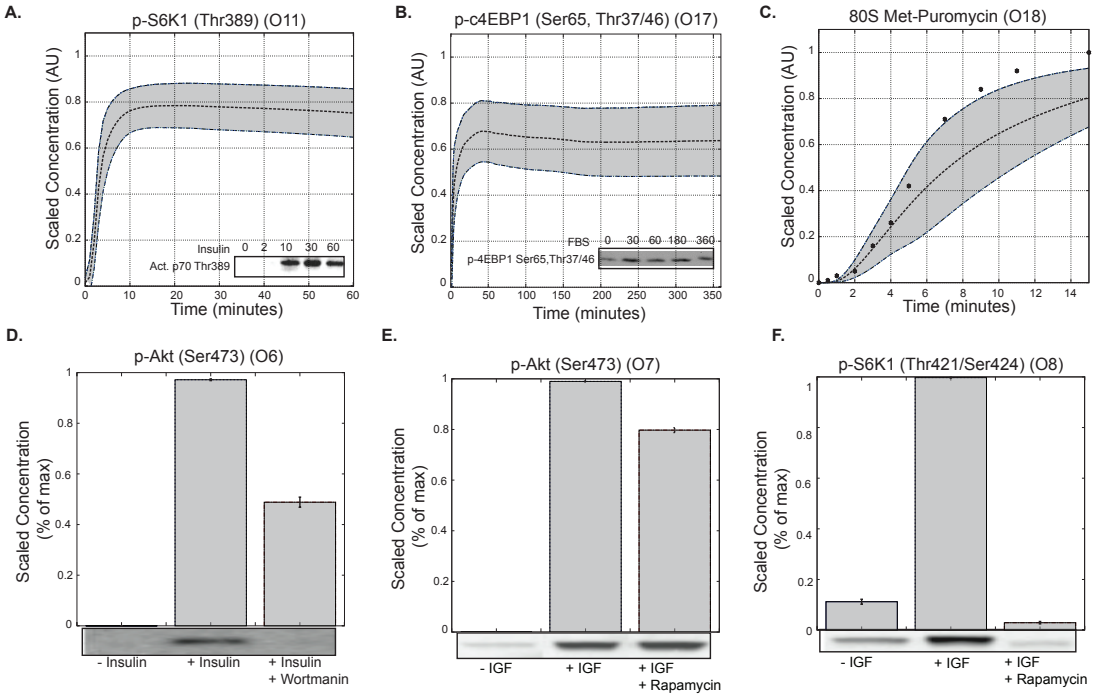

Figure 2.3: Ensemble Performance Against Training Data. Performance of each member of the model ensemble was compared against data. Dotted lines represent ensemble mean, shaded regions represent 99.9% confidence interval of deviation of mean. **A.** Time course data for p70S6K1 phosphorylation in response to insulin stimulation (L6 Myotubes) **B.** Time course data for c4EBP1 phosphorylation in response to FBS (RhoE 3T3 cells) **C.** In vitro time course of 80S complex measured by puromycin assay. (rabbit reticulocyte) **D.** pAkt(Ser473) levels at 20 minutes in the presence and absence of insulin and wortmanin, selective PI3K inhibitor. (393T cells) **E,F.** pAkt(Set473) and Activated p70S6K1 levels at 15 minutes in the presence and absence of insulin-like growth factor(IGF) and rapamycin, a selective mTOR inhibitor. (C2C12 myotubes)

increased Rheb-GTP activity. Garami *et al.* also measured the levels of GTP bound Rheb in both wild-type and TSC2 knockout cells. Because of TSC2's regulatory role in mediating Rheb-GTP levels, a TSC2 knockout had significantly increased Rheb-GTP levels ($\epsilon_{pred} = 0.10 \pm 0.03$, $\epsilon_{rand} = 0.09 \pm 0.06$) (Fig. 2.4C). Lastly, the model predicted the levels of 4E-BP1 bound eIF4E in response to heat shock ($\epsilon_{pred} = 0.51 \pm 0.33$, $\epsilon_{rand} = 1.67 \pm 1.17$) (Fig. 2.4D) [126]. Heat shock inhibits translation initiation through de-phosphorylation of 4E-BP1; because the model was not trained on stress-induced translation-inhibition, this result demonstrated the predictive power of the model population and the utility of using model populations for the prediction of the behavior of novel stimuli.

Table 2.2: Blind Prediction list along with species, cell-type, prediction error, random error with a randomly generated parameter set and the corresponding literature reference.

Prediction#	species	cell type	compartment	prediction	random	source
P1	43S-mRNA (GTP)	rabbit reticulocytes	in vitro	0.52 ± 0.40	0.82 ± 0.51	[66]
P2	Rheb-GTP	A14 NIH 3T3 cells	Total lysate	0.22 ± 0.11	0.42 ± 0.01	[34]
P3	Rheb-GTP	A14 NIH 3T3 cells	Total lysate	0.10 ± 0.03	0.09 ± 0.06	[34]
P4	eIF4E:4EBP1	CHO K1 cells	Total lysate	0.51 ± 0.33	1.67 ± 1.17	[126]
P5	pAkt(Ser473)	HEK293 cells	Total lysate	0.27 ± 0.09	0.72 ± 0.09	[34]

2.2.3 Sensitivity and robustness analysis identified robust and fragile features of the initiation architecture.

We generated falsifiable predictions about the fragility or robustness of structural features of the initiation architecture using sensitivity and robustness analysis. First order sensitivity coefficients were computed for 40 parameter sets

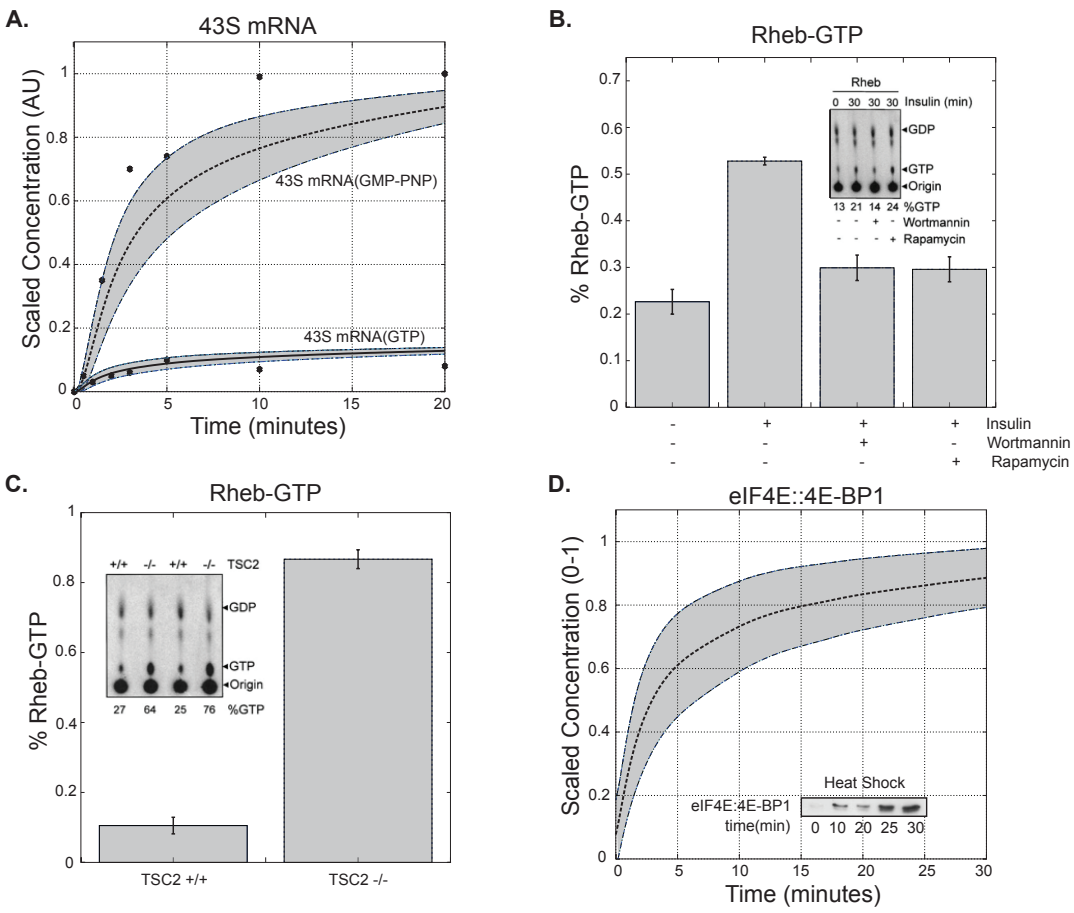

Figure 2.4: Model Predictions. Predictive ability of model ensemble was assessed by comparing model performance with novel experimental data. Dotted lines represent ensemble mean, shaded regions represent 99.9% confidence interval of deviation of mean. **A.** In vitro time course for formation of 43S-mRNA complex. A slowly-hydrolyzable GTP homologue(GMP-PNP) was used in place of GTP to isolate formation of this intermediate complex. GMP-PNP data was used for training while GTP data was used for validation. **B.** Percent of Rheb-GTP to Rheb-GDP in the presence of insulin, wortmanin and rapamycin.(A14 NIH 3T3 cells) **C.** Percent of Rheb-GTP to Rheb-GDP in wildtype and TSC2 lacking cells. (MEF cells) **D.** 4EBP1 bound EIF4E in the presence of heat shock.(CHO.K1 cells) .

selected from the ensemble (materials and methods), time-averaged and rank-ordered for the 250 species in the model, in the presence and absence of insulin and IRS-1 feedback. The sensitive components of insulin signaling shifted from Rheb in the absence of insulin to a combination of Rheb and PI3K in the presence of insulin. Sensitivity coefficients were calculated with and without insulin over the complete 100 min response (Fig. 2.5A). Globally, processes involved with 80S formation were consistently ranked among the most sensitive, irrespective of insulin. However, the sensitivity of other signal processing components changed with insulin status. For example, without insulin, Rheb/Rheb-GDP were highly fragile (NSS rank ≥ 0.25), while PI3K, PIP2, PIP3 and PTEN were highly robust (NSS rank ~ 0.0). Surprisingly, the relative sensitivity of these network components changed in the presence of insulin. While the fragility of Rheb/Rheb-GDP shifted upward with insulin, the sensitivity of PI3K and its downstream complexes increased dramatically (NSS rank ≥ 0.45) following insulin stimulation. This suggested that the combination of PI3K and Rheb activity was critical to insulin action over the full 100 min time window. However, it was unclear whether PI3K was always important, or if there was a temporal window in which PI3K became important following insulin stimulation. To explore this question, we time-averaged the sensitivity coefficients over early- and late-phase time periods following insulin stimulation (Fig. 2.5B). The 0-5 minute time period captured the initial network dynamics, while the 30-100 minute time period captured the network at a quasi-steady state. Generally, network components were more sensitive under dynamic operation (species beneath the 45^o line), compared with steady-state. However, there were exceptions to this trend. For example, PI3K, PTEN and TSC1/2 were equally sensitive in both time frames, suggesting these species played important roles in both dynamic

and steady-state signaling. On the other hand, the Rheb NSS rank decreased from 0.6 to 0.25 as the network moved toward steady-state. Taken together, the sensitivity results suggested that Rheb/Rheb-GDP activity controlled the background level of translation initiation while the PI3K axis in combination with Rheb/Rheb-GDP regulated insulin-induced initiation.

IRS1 phosphorylation, a well known negative feedback mechanism [67, 122, 121, 24], attenuated PI3K sensitivity. We explored the role of IRS1 feedback by comparing sensitivity coefficients under insulin stimulation in the presence and absence of IRS1 feedback (Fig. 2.5C). The most significant change without feedback was the sensitivity of the IR:IRS1 and adaptor complexes (Fig. 2.5C, black fill); IR:IRS1, which anchors the adaptor complex to the activated receptor and is immediately upstream of PI3K activation, changed from NSS rank $\simeq 0.04$ to 0.32. The sensitivity of the PI3K/Akt signaling axis also increased in the absence of feedback (Fig. 2.5C, grey fill). Surprisingly, the sensitivity of Rheb and many ribosomal components decreased in the absence of feedback. Similar results were observed when sensitivity coefficients were time averaged over the 0 to 5 min time window (Fig. 2.5D). These sensitivity calculations suggest that IRS1 feedback plays a significant role in insulin signaling by modulating the relative importance of PI3K versus Rheb. Thus, IRS1 feedback though not directly identified as a fragile regulatory motif, has significant effects on network function.

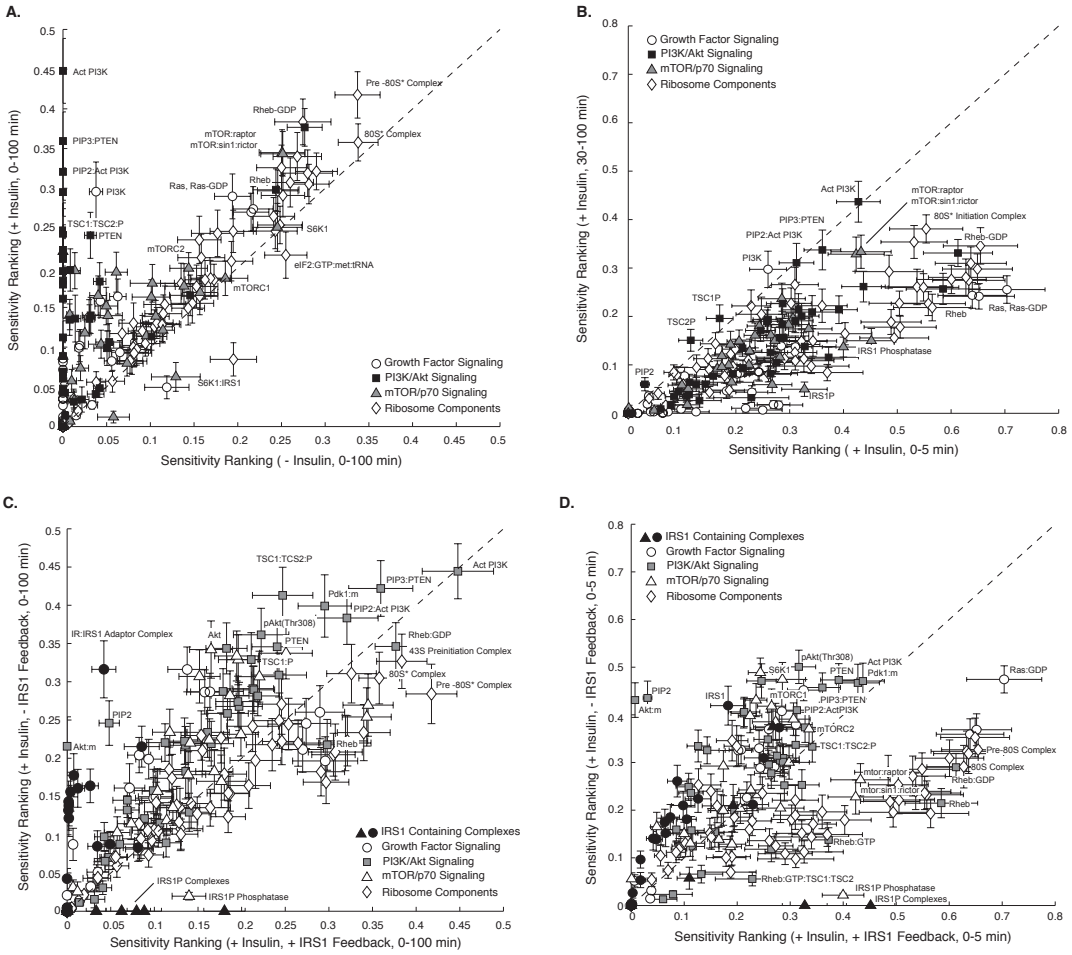

Figure 2.5: Sensitivity Analysis. Species with a high sensitivity ranking are considered fragile while species with a low sensitivity ranking are considered robust. **A.** Sensitivity ranking of network species in the presence and absence of insulin. **B.** Time-course Sensitivity ranking of network species. **C,D.** Sensitivity ranking of network species in the presence and absence of IRS1 feedback. Black fill represents complexes containing IRS1, Grey fill represents PI3K/Akt associated signaling. Sensitivity values were time averaged over 0-100 minutes and 0-5 minutes, respectively.

2.2.4 Robustness analysis identified key regulators of translation-initiation

Knockdown simulations were conducted for 92 proteins to estimate the functional connectedness of the initiation network. The effect of the perturbations were quantified by calculating the fold change in translational activity (α) for each simulated knockout in the presence (Fig. 2.6A) and absence (Fig. 2.6B) of insulin. Knockdown simulations were conducted using 400 models selected from the ensemble based on CV and correlation (materials and methods). Sensitivity analysis suggested basal translation was governed by Rheb, while insulin-induced initiation was governed by PI3K. Robustness analysis showed that perturbations in PI3K signaling, in the presence of insulin, restored initiation control to Rheb. Proteins were classified based on their impact on translational activity: little or no effect ($\alpha \approx 1$, white fill), moderate decrease ($\alpha \approx 0.6$, dark grey), critical ($\alpha \approx 0$, light grey) and increase ($\alpha > 1$, black). Generally, knockdowns in the presence of insulin were more likely to decrease initiation (Fig. 2.6A). Knockdown analysis identified 24 proteins (or 26% of the network) that were critical to translation initiation irrespective of insulin status; these critical components included mTORC1, S6K1, several initiation factors and other ribosomal components. Initiation was moderately reduced by disrupting species immediately upstream or downstream of PI3K; a moderate reduction in the presence of insulin further demonstrates that initiation is governed by both PI3K and Rheb. Lastly, deletion of TSC1/2 (negative regulator of Rheb) or 4E-BP1 (sequesters the cap-binding protein eIF4E), increased initiation in the presence of insulin. Interestingly, for several proteins the direction or magnitude of change in initiation activity depended upon the presence or absence of insulin. For example,

PTEN deletion significantly increased initiation ($\alpha \gg 1$) in the absence of insulin, but had no effect when insulin was present. On the other hand, PI3K deletion had a moderate reduction in the presence of insulin, but only a small effect in the absence of insulin (Fig. 2.6B). These results suggested that PI3K and PTEN were conditionally fragile proteins; in the presence of insulin, PI3K is critical signal processing node, while PTEN acts to restrain inadvertent basal initiation. We further tested this hypothesis by exploring a Rheb knockdown. Our expectation from sensitivity analysis was that a Rheb knockdown would reduce initiation, irrespective of insulin status. However, paradoxically, Rheb and mTORC2 subunit (sin1, rictor) knockdowns increased initiation.

We explored this result by examining the behavior of each individual member of the ensemble (Fig. 2.6C). Following the deletion of PTEN, approximately 80% (or 323 of the 400 models sampled) had increased initiation in the absence of insulin. Of these models, 16% (or 51 of 323) had at least a two fold increase in translational activity. This result was expected, deletion of a protein species resulted in a qualitatively similar change in initiation across the ensemble of models. However, for Rheb knockdowns, members of the ensemble demonstrated qualitatively different behavior. For 84% (or 334 of 400) of the models sampled, Rheb knockdowns significantly down-regulated initiation. Thus, the vast majority of models behaved as expected. Interestingly, 20 models (or 5% of the models sampled) had increased translation initiation in the presence of a Rheb knockdown, with 15 models demonstrating greater than a two-fold change (Fig. 2.6C). Thus, the model population estimated by POETs, contained models that showed qualitatively different behavior. Histograms of sin1 and rictor knockdowns showed a similar trend (results not shown). To explore this population heterogeneity, we isolated parameter sets demonstrating contrasting qualitative

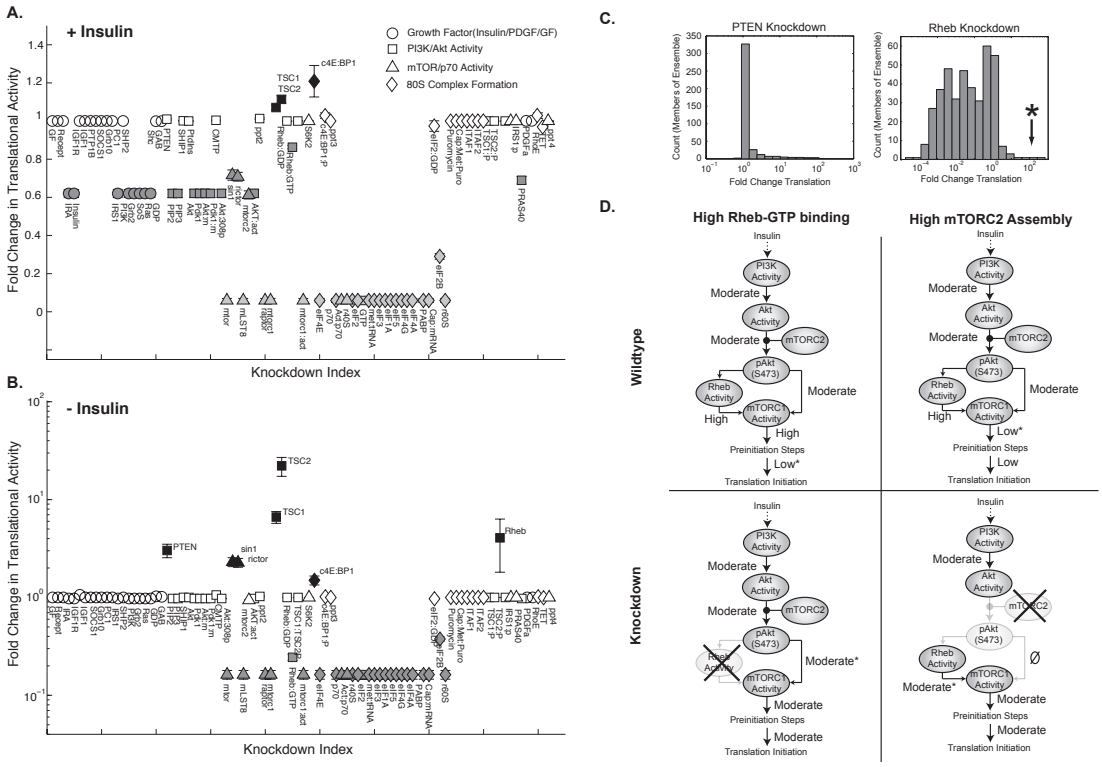

Figure 2.6: Species Knockdowns. Simulated knockdowns were performed by removing nodes from the stoichiometric matrix. The fold-change in expression levels resulting from perturbations quantified the impact of each knockdown. Calculations were performed on all 400 members of the ensemble. **A.** Species knockdowns in the presence of insulin. Simulated knockdowns resulted in increased (black), constant (white), a moderately decreased (dark grey) or a severely decreased (light grey) translational levels. **B.** Species knockouts in the absence of insulin. Simulated knockdowns resulted in increased (black), constant (white), or decreased (grey) translational levels. **C.** Histogram of translation levels across each member of parameter ensemble. Asterisk indicates parameter sets that were selected for further analysis. **D.** Alternative modes of network operation. For a subset of the ensemble, the network demonstrates operational modes that can result in translation increases upon Rheb or mTORC2 disruption. Asterisk indicates rate-limiting step.

behavior. We explored flux vectors of these outlying parameter sets to better understand the mechanistic effect of Rheb and rictor/sin1 knockouts. All of the outlying models were in regions of parameter space where the association between Rheb and GTP were very high. Strong Rheb/GTP binding resulted in abnormally high signal flux to mTORC1 despite the inhibitory effects of TSC1/2 (Fig. 2.6D, top-left). Consequently, less GTP was available for the energy-dependent steps of translation initiation (i.e. formation of eIF2-GTP-met-tRNA tertiary complex). Additionally, strong association between Rheb and GTP resulted in high levels of activated mTORC1 and S6K1. However, despite the high levels of mTORC1, GTP-dependent pre-initiation reactions were rate limiting (Fig. 2.6D, labeled*). Thus, Rheb knockdown released the network from its GTP limitation and shifted the predominant signaling mode to mTORC2. This shift in signaling, while lowering the activated mTORC1/S6K1 level, ultimately resulted in higher levels of initiation (Fig. 2.6 bottom-left). On the other hand, the rictor/sin1 knockdown behaved differently. The rate-limiting step for the rictor/sin1 knockdowns was mTORC1 activation: more Rheb-GTP was present than there was mTORC1 to be activated (Fig. 2.6D top-right). Thus, knockdown of rictor/sin1 prevented the assembly of mTORC2 and freed the mTOR subunit to be used for mTORC1 assembly. This shift toward mTORC1 assembly and activation relieved the Rheb-GTP/mTORC1 bottleneck, resulting in increased initiation.

2.3 Discussion

In this study we developed and analyzed a population of insulin- and growth-factor induced translation initiation models. These models described the inte-

gration of insulin and growth-factor signals with 80S assembly. We addressed parametric uncertainty by identifying an uncorrelated population of parameter sets consistent with 24 transient and steady-state data sets using multiobjective optimization. The model family also predicted novel data sets not used during model training. The population of initiation models was analyzed using sensitivity and robustness analysis to identify the key components of insulin-induced translation initiation. Without insulin, a balance between the pro-initiation activity of the GTP-binding protein Rheb and anti-initiation activity of PTEN controlled basal initiation. Rheb knockdown simulations confirmed decreased initiation in the majority of the model population. Surprisingly, we also identified a model subpopulation in which deletion of Rheb or mTORC2 components increased initiation. In these cases, removal of Rheb or mTORC2 components relieved a rate-limiting bottleneck e.g., constrained levels of GTP, leading to increased initiation. On the other hand, in the absence of insulin, translation initiation increased for all models in the population following a PTEN deletion. In the presence of insulin, Rheb and PTEN were no longer the dominant arbiters of initiation; a combination of PI3K and Rheb activity controlled inducible initiation, where PI3K was only critical in the presence of insulin. PI3K deletion in the presence of insulin removed the ability of the network to process insulin signals, but did not remove initiation altogether. PI3K deletion reduced initiation to approximately 60% of its maximum level. Interestingly, the relative contribution of PI3K versus Rheb to the overall initiation level could be tuned by controlling the level of IRS1 feedback. In the absence of feedback, PI3K was more important than Rheb to signal propagation, while the opposite was true in the presence of feedback.

Our study identified an insulin-dependent switch that controlled transla-

tion initiation. In the absence of insulin, initiation was controlled by a balance between the pro-initiation activity of Rheb-GTP and the anti-initiation activity of PTEN. Upon insulin stimulation, control of signaling shifted from PTEN to PI3K. The cellular decision to choose either operational mode was highly fragile. Perturbation of network components was observed to switch the network between pro- and anti-initiation modes. This paradigm is useful towards understanding various disease states. *Yuan and Cantley* have noted that every major species in the PI3K pathway is mutated or over-expressed in a wide variety of solid tumors [131]. Mutations in PIK3CA, the gene encoding the catalytic subunit of PI3K, has been shown to induce oncogene signaling in human cancers by causing constitutive PI3K signaling [93]. PTEN mutations have also been implicated in a wide variety of cancers [90]. Both PIK3CA and PTEN mutations induce a pro-initiation operational mode in the absence of growth factor. Further, enhancement of Rheb activity can also induce a pro-initiation mode. Saucedo *et al.* showed that Rheb over-expression resulted in increased translation, even in the absence of insulin or other growth factors [98]. Malfunctions in Rheb signaling in the form of both Rheb and TSC1/2 mutations are also frequently observed in cancer [53, 64]. Our analysis suggests that all such malfunctions are all due to a wrongly activated initiation program. We claim that the mechanistic basis of these malfunctions lies at the intersection of Rheb, PTEN and PI3K mediated control. Our findings support the findings of Taniguchi *et al.* and the identification of PI3K as a critical node in the insulin signaling network [116]. Importantly however, we have shown that the role of PI3K is nuanced . Whereas insulin-signaling was controlled by PI3K and Rheb-GTP, basal initiation was controlled by a fragile balance between the induction of Rheb-GTP and the restraint of PTEN.

Though the initiation model was assembled from an extensive literature review, several potentially important signaling mechanisms were not included. First, we should revisit the role PRAS40. Currently, PRAS40 acts as a cofactor that aids in pAkt (Ser473)-mediated activation of mTORC1. Sancak *et al* suggested that PRAS40 sequesters mTORC1, and only after phosphorylation by Akt releases from mTORC1 [94]. Other groups have also shown that mTORC1 can phosphorylate and inhibit PRAS40, thus providing a positive-feedback mechanism for Akt-mediated mTORC1 activation [30, 127]. A more complete description of PRAS40 will enhance our ability to interrogate Akt dependent mTORC1 activation. Second, we need to refine the description of IRS1 feedback. Currently, we assume a single deactivating phosphorylation event at Ser308. However, several studies have shown that IRS1 can be phosphorylated at multiple serine sites, which are both activating and deactivating [79, 37]. Additionally, PTEN is known to dephosphorylate activated Platelet-derived Growth Factor (PDGF) receptors and attenuate their activity, a feature not included currently [114]. A more complete description of IRS1 phosphorylation could help define how (and under what conditions) IRS1 regulation attenuates PI3K activation. Third, we modeled the regulation of 4E-BPx as a single phosphorylation event where phosphorylated 4E-BPx was unable to bind to eIF4E. In reality, 4E-BPx family members, such as 4E-BP1, have several phosphorylation sites [81] and the release of eIF4E is driven only after multiple conserved phosphorylation events [36]. Additionally, eIF4E can itself be phosphorylated at Ser209; while there is agreement that the phosphorylation of eIF4E does have a regulatory significance, the data is contradictory as to whether it is positive or negative [100]. Fourth, signaling downstream of mTORC1 has also been shown to mediate translation modes beyond those included in our model. eIF3 has been iden-

tified as a scaffolding protein that recruits mTORC1 to untranslated mRNA and facilitates S6K1 and 4E-BP1 phosphorylation [45]. S6K1 can also activate eIF4B, a protein that helps eIF4A to unwind the secondary structure of untranslated mRNA [82]. Further, a recently discovered scaffold protein, SKAR, has been shown to assist S6K1 recruitment to mRNA [68]. Lastly, because of mTORC1's unique role in cellular metabolism it would be interesting to explore how other aspects of metabolism interact with insulin signaling to mediate decisions between translation, lipid synthesis and proliferation.

2.4 Materials and Methods

2.4.1 Formulation and solution of the model equations.

The translation initiation model was formulated as a set of coupled non-linear ordinary differential equations (ODEs):

$$\frac{d\mathbf{x}}{dt} = \mathbf{S} \cdot \mathbf{r}(\mathbf{x}, \mathbf{p}) \qquad \mathbf{x}(t_o) = \mathbf{x}_o \tag{2.1}$$

The symbol $\mathbf{S}$ denotes the stoichiometric matrix (250×573). The quantity $\mathbf{x}$ denotes the concentration vector of proteins (250×1). The term $\mathbf{r}(\mathbf{x}, \mathbf{p})$ denotes the vector of reaction rates (573×1). Each row in $\mathbf{S}$ described a protein, while each column described the stoichiometry of network interactions. Thus, the (i, j) element of $\mathbf{S}$, denoted by σ_{ij}, described how protein i was involved in rate j. If $\sigma_{ij} < 0$, then protein i was consumed in r_j. Conversely, if $\sigma_{ij} > 0$, protein i was produced by r_j. Lastly, if $\sigma_{ij} = 0$, then protein i was not involved in rate j.

We assumed mass-action kinetics for each interaction in the network. The rate expression for interaction q was given by:

$$r_q\left(\mathbf{x}, k_q\right) = k_q \prod_{j \in \{\mathbf{R}_q\}} x_j^{-\sigma_{jq}} \tag{2.2}$$

The set $\left\{\mathbf{R}_q\right\}$ denotes reactants for reaction q while σ_{jq} denotes the stoichiometric coefficient (element of the matrix $\mathbf{S}$) governing species j in reaction q. All reversible interactions were split into two irreversible steps. The mass-action formulation, while expanding the dimension of the initiation model, regular-

ized the mathematical structure; this allowed automatic generation of the model code using UNIVERSAL and regularized the unknown model parameters (parameters were one of only three types, association, dissociation or catalytic rate constants). UNIVERSAL, an open source Objective-C/Java code generator which generates model code from text and SBML inputs, is freely available as a Google Code project (http://code.google.com/p/universal-code-generator/). The model equations were solved using the LSODE routine in OCTAVE (v 3.0.5; www.octave.org) on an Apple workstation (Apple, Cupertino, CA; OS X v10.6.4).

When calculating the response of the model to the addition of insulin or other growth factors, we first ran to steady-state and then issued the perturbation. The steady-state was estimated numerically by repeatedly solving the model equations and estimating the difference between subsequent time points:

$$\|\mathbf{x}(t + \Delta t) - \mathbf{x}(t)\|_2 \leq \gamma \tag{2.3}$$

The quantities $\mathbf{x}(t)$ and $\mathbf{x}(t + \Delta t)$ denote the simulated concentration vector at time t and $t + \Delta t$, respectively. The L_2 vector-norm was used as the distance metric, where $\Delta t = 1$ s and $\gamma = 0.001$ for all simulations.

2.4.2 Estimation and cross-validation of a population of models using Pareto Optimal Ensemble Techniques (POETs).

POETs is a multiobjective optimization strategy which integrates several local search strategies e.g., Simulated Annealing (SA) or Pattern Search (PS) with a

Pareto-rank-based fitness assignment [107]. Denote a candidate parameter set at iteration $i + 1$ as $\mathbf{k}_{i+1}$. The squared error for $\mathbf{k}_{i+1}$ for training set j was defined as:

$$E_j(\mathbf{k}) = \sum_{i=1}^{\mathcal{T}_j} \left(\hat{\mathcal{M}}_{ij} - \hat{y}_{ij}(\mathbf{k}) \right)^2 \tag{2.4}$$

The symbol $\hat{\mathcal{M}}_{ij}$ denotes scaled experimental observations (from training set j) while the symbol $\hat{y}_{ij}$ denotes the scaled simulation output (from training set j). The quantity i denotes the sampled time-index and $\mathcal{T}_j$ denotes the number of time points for experiment j. The read-out from the training immunoblots was band intensity estimated using the ImageJ software package. The scaled measurement for species x at time $i = \{t_1, t_2, .., t_n\}$ in condition j is given by:

$$\hat{\mathcal{M}}_{ij} = \frac{\mathcal{M}_{ij} - \min_i \mathcal{M}_{ij}}{\max_i \mathcal{M}_{ij} - \min_i \mathcal{M}_{ij}} \tag{2.5}$$

Under this scaling, the lowest intensity band equaled zero while the highest intensity band equaled one. A similar scaling was defined for the simulation output.

We computed the Pareto rank of $\mathbf{k}_{i+1}$ by comparing the simulation error at iteration $i+1$ against the simulation archive $\mathbf{K}_i$. We used the Fonseca and Fleming ranking scheme [31]:

$$rank\,(\mathbf{k}_{i+1} \mid \mathbf{K}_i) = p \tag{2.6}$$

where p denotes the number of parameter sets that dominate parameter set $\mathbf{k}_{i+1}$. Parameter sets on or near the optimal trade-off surface have small rank. Sets with increasing rank are progressively further away from the optimal trade-off surface. The parameter set $\mathbf{k}_{i+1}$ was accepted or rejected by the SA with

probability $\mathcal{P}(\mathbf{k}_{i+1})$:

$$\mathcal{P}(\mathbf{k}_{i+1}) \equiv \exp\{-rank(\mathbf{k}_{i+1} \mid \mathbf{K}_i)/T\} \tag{2.7}$$

where T is the computational annealing temperature. The initial temperature $T_o = n/log(2)$, where n is user defined ($n = 4$ for this study). The final temperature was $T_f = 0.1$. The annealing temperature was discretized into 10 quanta between T_o and T_f and adjusted according to the schedule $T_k = \beta^k T_0$ where β was defined as:

$$\beta = \left(\frac{T_f}{T_o}\right)^{1/10} \tag{2.8}$$

The epoch-counter k was incremented after the addition of 100 members to the ensemble. Thus, as the ensemble grew, the likelihood of accepting parameter sets with a large Pareto rank decreased. To generate parameter diversity, we randomly perturbed each parameter by $\leq \pm 25\%$. We performed a local pattern-search every q steps to minimize the residual for a single randomly selected objective. The local pattern-search algorithm has been described previously [33, 123]. The parameter ensemble used in the simulation and sensitivity studies was generated from the low-rank parameter sets in $\mathbf{K}_i$.

A leave-three-out cross-validation strategy was used to simultaneously calculate the training and prediction error during the parameter estimation procedure [60]. The 24 training data sets were partitioned into eight subsets, each containing 21 data sets for training and three data sets for validation. The leave-three-out scheme generated 18,886 probable models, from which we selected a subset for further study. From the rank zero models, we iteratively selected 50 random models from each cross-validation trial with the lowest correlation

and shortest euclidian distance to the origin (minimum error). This selection technique produced sub-ensembles with low set-to-set correlation (≤ 0.50) and minimum training error.

2.4.3 Sensitivity and robustness analysis of the initiation model population.

Sensitivity coefficients were calculated as shown previously [108, 107, 117] for 40 models selected from the ensemble (rank-zero, low-correlation, minimum error selection). The resulting sensitivity coefficients were scaled and time-averaged (Trapezoid rule):

$$\mathcal{N}_{ij} \equiv \frac{1}{T} \int_0^T dt \cdot |\alpha_{ij}(t)\, s_{ij}(t)| \tag{2.9}$$

where T denotes the final simulation time and $\alpha_{ij} = 1$. The time-averaged sensitivity coefficients were then organized into an array for each ensemble member:

$$\mathcal{N}^{(\epsilon)} = \begin{pmatrix} \mathcal{N}_{11}^{(\epsilon)} & \mathcal{N}_{12}^{(\epsilon)} & \dots & \mathcal{N}_{1j}^{(\epsilon)} & \dots & \mathcal{N}_{1P}^{(\epsilon)} \\ \mathcal{N}_{21}^{(\epsilon)} & \mathcal{N}_{22}^{(\epsilon)} & \dots & \mathcal{N}_{2j}^{(\epsilon)} & \dots & \mathcal{N}_{2P}^{(\epsilon)} \\ \vdots & \vdots & & \vdots & & \vdots \\ \mathcal{N}_{M1}^{(\epsilon)} & \mathcal{N}_{M2}^{(\epsilon)} & \dots & \mathcal{N}_{Mj}^{(\epsilon)} & \dots & \mathcal{N}_{MP}^{(\epsilon)} \end{pmatrix} \qquad \epsilon = 1, 2, \dots, N_\epsilon \tag{2.10}$$

where ϵ denotes the index of the ensemble member, P denotes the number of parameters, N_ϵ denotes the number of ensemble samples and M denotes the number of model species. To estimate the relative fragility or robustness of species and reactions in the network, we decomposed the $\mathcal{N}^{(\epsilon)}$ matrix using Singular

Value Decomposition (SVD):

$$\mathcal{N}^{(\epsilon)} = \mathbf{U}^{(\epsilon)}\Sigma^{(\epsilon)}\mathbf{V}^{T,(\epsilon)} \tag{2.11}$$

Coefficients of the left (right) singular vectors corresponding to largest β singular values of $\mathcal{N}^{(\epsilon)}$ were rank-ordered to estimate important species (reaction) combinations. Only coefficients with magnitude greater than a threshold (δ = 0.001) were considered. The fraction of the β vectors in which a reaction or species index occurred was used to rank its importance.

Robustness coefficients were calculated as shown previously [118]. Robustness coefficients (denoted by $\alpha\left(i, j, t_o, t_f\right)$) are the ratio of the integrated concentration of a network marker in the presence (numerator) and absence (denominator) of structural or operational perturbation. The quantities t_0 and t_f denote the initial and final simulation time respectively, while i and j denote the indices for the marker and the perturbation respectively. If $\alpha\left(i, j, t_o, t_f\right) > 1$, then the perturbation *increased* the marker concentration. Conversely, if $\alpha\left(i, j, t_o, t_f\right) \ll 1$ the perturbation *decreased* the marker concentration. Lastly, if $\alpha\left(i, j, t_o, t_f\right) \sim 1$ the perturbation did not influence the marker concentration. The $\alpha\left(i, j, t_o, t_f\right)$ were calculated over 400 models selected from the ensemble (rank-zero, low-correlation, minimum error selection).

CHAPTER 3

SUMMARY AND FUTURE DIRECTIONS

In the previous sections we have developed a mathematical model of eukaryotic translation initiation. We have used this model to identify the important network components under basal and insulin-induced signaling. We have also analyzed the ability of the system to respond to various network perturbations. Our observations correspond to those observed in vitro and can be used to clarify disease states associated with insulin-mediated translation initiation malfunction.

As stated previously, mechanistic models are used to gain insight into the dynamics and function of complex biological systems. As systems become increasingly complex, mechanistic models become an irreplaceable tool towards understanding network function. Yet, understanding complex systems requires models and computational tools to become equally complex. If biologists and engineers hope to understand some of the most complex biological systems, models must become larger and analytical tools must improve. Models must incorporate more pathways, more signaling events, more ligands, and more regulatory components in order to truly capture the complexity of biological behavior. Systems biology must integrate up the length scale, towards the scale of cells, tissues, organs or entire organisms. Both the models and the scope of measurement must increase. Systems biologists must echo the timeless conclusion of every man who is stuck at the bottom of a well, "the only way out is up".

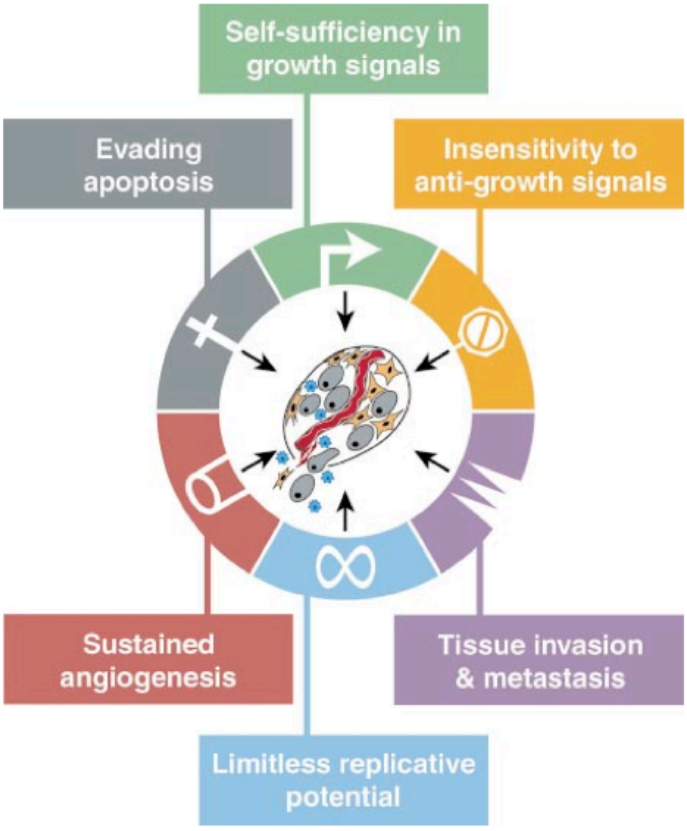

Figure 3.1: The Hallmarks of Cancer. Used from *Hanahan and Weinberg*, 2000 [39]

3.1 Translation initiation in cancer

One direction of model expansion is in the realm of cancer. Of all biological systems, cancer is the most infamous for its immense complexity. The emergence of cancer is marked by numerous hallmarks such as insensitivity to anti-growth signals, limitless replicative potential, sustained angiogenesis and metastasis (Fig. 3.1) [39]. Understanding the signaling underlying these phenotypes is not a trivial task. Mathematical models will be irreplaceable as researchers try to investigate how these phenotypes arise from both genotype and external stimuli upon the cell.

The Varner Laboratory has several publications and current projects investigating aspects of the cancer phenotype. Mathematical models have been published on prostate cancer, cell-cycle and apoptosis [117, 76, 32] with current projects investigating angiogenesis, breast cancer, and TNFα signaling. Integration of these models together, will provide a useful framework for interrogating the exact mechanisms and pathways that can lead to cancer.

Such integration however, is far from trivial. As models become larger, problems of parameter identifiability and model validation abound. Further, advanced computational methods and faster mathematical solvers are imperative for model development and analysis. Models of this size also place a premium of high-quality quantitative data that can be used to train a model accurately.

3.2 Metabolic regulation

mTOR has long been recognized as a nutrient sensor and a regulator of growth. In addition to translation-initiation, mTOR is associated with numerous methods of nutrient sensing and regulation (Fig. 3.2). Amino-acids and glucose can also induce mTOR activity [133]. mTOR has also been shown to upregulate genes associated with lipid synthesis, metabolism, proliferation and apoptosis [133]. Incorporation of these pathways could help to understand how mTOR regulates diverse metabolic pathways.

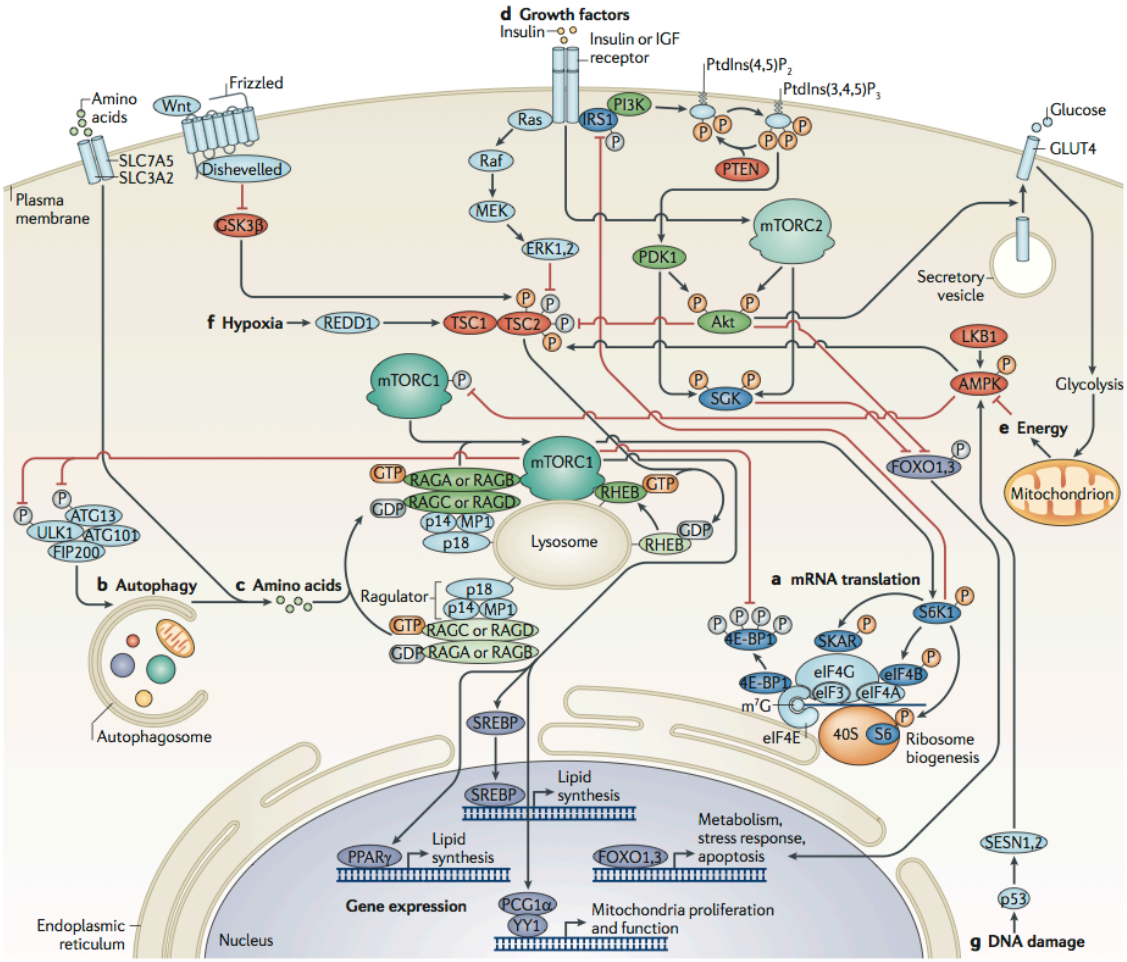

Figure 3.2: The mTOR Signaling Pathway. Used from *Zoncu et al.* 2010 [133]

3.3 Final Thoughts

Systems biology has seen huge advancements in the past decade. It has grown from an offshoot of molecular biology into a field of its own. Systems biology now has its own conferences, research centers and academic departments. Yet these strides forward have been met with new challenges. Researchers have recognized that quality of data is favored over quantity of data and have be-

gun to develop more accurate 'omics' technologies. Further, the difficulties of systems approaches has constrained the fields growth. Kitano states it simply, "Genomics exploded, because if you buy a sequencing machine, anyone can do it. But having to combine good biology with good mathematical modeling isn't easy" [69].

Nonetheless, systems biology continues to move forward. In a recent essay in the biological journal *Cell*, Adam Arkin and David Schaffer conclude,

> *"As systems biology matures, the number of studies linking correlation with causation and principles with prediction continues to grow... Advances in measurement technologies that enable large-scale experiments across an array of parameters and conditions will increasingly meld these correlative and causal approaches, including correlative analyses leading to mechanistic hypothesis testing as well as causal models empowered with sufficient data to make predictions... The increasing integration of experimental and computational technologies will thus corroborate, deepen, and diversify the theories that the earliest systems biologists used logic to infer, thereby inching us ever closer to that central question: "What is Life"?"* [3]

Even seventy years later, the timeless question of Erwin Schrödinger remains. How do we explain our own existence? How does our simple genetic code result in what we commonly refer to as life? I expect that these questions will never be fully answered to our satisfaction. Reflections on the purpose and meaning of life have have intrigued theologians and philosophers for millennia. Yet, that should not deter us from investigation. We've been given the tools to explore, perhaps its about time we get back to digging.

APPENDIX A

ABBREVIATIONS

Table A.1: Abbreviations and Species Names

Abbreviation	Species Name
IGF1	Insulin-like Growth Factor 1
IGF1R	Insulin-like Growth Factor Receptor
IRA	Insulin Receptor
SHP2	SH2-domain-containing tyrosine phosphatase-2
Grb2	growth-factor-receptor-bound protein-2
Shc	Src-homology-2-containing protein
SoS	son-of-sevenless
SOCS1/3	suppressor of cytokine signaling-1/3
PTP1B	protein tyrosine phosphatase-1B
Grb10	growth-factor-receptor-bound protein 10
PC1	plasma-cell-membrane glycoprotein-1
IRS1	insulin-receptor substrate 1
pIRS1	inhibitory IRS1 phosphorylation
PTEN	phosphatase and tensin homologue
PIP2	0hosphatidylinositol 4,5-bisphosphate
PIP3	phosphatidylinositol-3,4,5-triphosphate
PI3K	Phosphatidylinositol 3-kinase
Pdk1	phosphoinositide-dependent kinase 1
Pdk1:m	Membrane-associated Pdk1
Akt:m	Membrane-associated Akt
pAkt(Thr308)	Phosphorylated Akt(Thr308)
pAkt(Ser473)	Phosphorylated Akt(Ser473)
rictor	rapamycin-insensitive companion of mTOR
SIN1	mammalian stress-activated map kinase-interacting protein 1

mLST8	mammalian lethal with SEC13 protein 8
mTOR	mammalian target of rapamycin
mTORC2	mTOR complex 2
TSC1/2	tuberous sclerosis 1/2 complex
pTSC1/2	inhibitory TSC1/2 phosphorylation
raptor	regulatory associated protein of mTOR
Rheb	Ras homologue enriched in brain
mTORC1	mTOR complex 1
4E-BP1	eIF4E-binding protein 1
eIF4E	eukaryotic translation initiation factor 4E
S6K1	S6 kinase 1
pS6K1	Activated S6K1 phosphorylation
eIFx	eukaryotic translation initiation factor
PABP	Poly(A) binding protein
AUG	initiation codon
40S	40S ribosomal subunit
1	eukaryotic translation initiation factor 1
met-tRNA	anticodon loop of initiator tRNA
GDP	Guanosine diphosphate
GTP	Guanosine triphosphate

BIBLIOGRAPHY

[1] Alan Aderem. Systems biology: its practice and challenges. *Cell*, 121(4):511–513, May 2005.

[2] U. Alon, M. G. Surette, N. Barkai, and S. Leibler. Robustness in bacterial chemotaxis. *Nature*, 397(6715):168–171, Jan 1999.

[3] Adam P Arkin and David V Schaffer. Network news: innovations in 21st century systems biology. *Cell*, 144(6):844–849, Mar 2011.

[4] O. T. Avery, C. M. Macleod, and M. McCarty. INDUCTION OF TRANSFORMATION BY A DESOXYRIBONUCLEIC ACID FRACTION ISOLATED FROM PNEUMOCOCCUS TYPE III. *J Exp Med*, 79(2):137–158, Feb 1944.

[5] Ziv Bar-Joseph, Georg K Gerber, Tong Ihn Lee, Nicola J Rinaldi, Jane Y Yoo, Franois Robert, D. Benjamin Gordon, Ernest Fraenkel, Tommi S Jaakkola, Richard A Young, and David K Gifford. Computational discovery of gene modules and regulatory networks. *Nat Biotechnol*, 21(11):1337–1342, Nov 2003.

[6] N. Barkai and S. Leibler. Robustness in simple biochemical networks. *Nature*, 387(6636):913–917, Jun 1997.

[7] John M S Bartlett and David Stirling. A short history of the polymerase chain reaction. *Methods Mol Biol*, 226:3–6, 2003.

[8] Arrigo De Benedetti and Jeremy R Graff. eIF-4E expression and its role in malignancies and metastases. *Oncogene*, 23(18):3189–3199, Apr 2004.

[9] Mary-Ann Bjornsti and Peter J Houghton. Lost in translation: dysregulation of cap-dependent translation and cancer. *Cancer Cell*, 5(6):519–523, Jun 2004.

[10] Nikolay Borisov, Edita Aksamitiene, Anatoly Kiyatkin, Stefan Legewie, Jan Berkhout, Thomas Maiwald, Nikolai P Kaimachnikov, Jens Timmer, Jan B Hoek, and Boris N Kholodenko. Systems-level interactions between insulin-EGF networks amplify mitogenic signaling. *Mol Syst Biol*, 5:256, 2009.

[11] Michael J Buck and Jason D Lieb. ChIP-chip: considerations for the design, analysis, and application of genome-wide chromatin immunoprecipitation experiments. *Genomics*, 83(3):349–360, Mar 2004.

[12] Eugene C Butcher. Can cell systems biology rescue drug discovery? *Nat Rev Drug Discov*, 4(6):461–467, Jun 2005.

[13] Eugene C Butcher, Ellen L Berg, and Eric J Kunkel. Systems biology in drug discovery. *Nat Biotechnol*, 22(10):1253–1259, Oct 2004.

[14] Gareth Butland, Jos Manuel Peregrn-Alvarez, Joyce Li, Wehong Yang, Xiaochun Yang, Veronica Canadien, Andrei Starostine, Dawn Richards, Bryan Beattie, Nevan Krogan, Michael Davey, John Parkinson, Jack Greenblatt, and Andrew Emili. Interaction network containing conserved and essential protein complexes in Escherichia coli. *Nature*, 433(7025):531–537, Feb 2005.

[15] J. M. Carlson and John Doyle. Complexity and robustness. *Proc Natl Acad Sci U S A*, 99 Suppl 1:2538–2545, Feb 2002.

[16] Etienne Caron, Samik Ghosh, Yukiko Matsuoka, Dariel Ashton-Beaucage, Marc Therrien, Sbastien Lemieux, Claude Perreault, Philippe P Roux, and Hiroaki Kitano. A comprehensive map of the mTOR signaling network. *Mol Syst Biol*, 6:453, Dec 2010.

[17] M. Chee, R. Yang, E. Hubbell, A. Berno, X. C. Huang, D. Stern, J. Winkler, D. J. Lockhart, M. S. Morris, and S. P. Fodor. Accessing genetic information with high-density DNA arrays. *Science*, 274(5287):610–614, Oct 1996.

[18] William W Chen, Birgit Schoeberl, Paul J Jasper, Mario Niepel, Ulrik B Nielsen, Douglas A Lauffenburger, and Peter K Sorger. Input-output behavior of ErbB signaling pathways as revealed by a mass action model trained against dynamic data. *Mol Syst Biol*, 5:239, 2009.

[19] S. N. Cohen, A. C. Chang, H. W. Boyer, and R. B. Helling. Construction of biologically functional bacterial plasmids in vitro. *Proc Natl Acad Sci U S A*, 70(11):3240–3244, Nov 1973.

[20] Michael E Cusick, Niels Klitgord, Marc Vidal, and David E Hill. Interactome: gateway into systems biology. *Hum Mol Genet*, 14 Spec No. 2:R171–R181, Oct 2005.

[21] Stephen G Dann, Anand Selvaraj, and George Thomas. mTOR Complex1-S6K1 signaling: at the crossroads of obesity, diabetes and cancer. *Trends Mol Med*, 13(6):252–259, Jun 2007.

[22] K. Danna and D. Nathans. Specific cleavage of simian virus 40 DNA by restriction endonuclease of Hemophilus influenzae. *Proc Natl Acad Sci U S A*, 68(12):2913–2917, Dec 1971.

[23] Richard J Dimelow and Stephen J Wilkinson. Control of translation initiation: a model-based analysis from limited experimental data. *J R Soc Interface*, 6(30):51–61, Jan 2009.

[24] John B Easton, Raushan T Kurmasheva, and Peter J Houghton. IRS-1: auditing the effectiveness of mTOR inhibitors. *Cancer Cell*, 9(3):153–155, Mar 2006.

[25] M. Elchebly, P. Payette, E. Michaliszyn, W. Cromlish, S. Collins, A. L. Loy, D. Normandin, A. Cheng, J. Himms-Hagen, C. C. Chan, C. Ramachandran, M. J. Gresser, M. L. Tremblay, and B. P. Kennedy. Increased insulin sensitivity and obesity resistance in mice lacking the protein tyrosine phosphatase-1B gene. *Science*, 283(5407):1544–1548, Mar 1999.

[26] Jeffrey A Engelman. Targeting PI3K signalling in cancer: opportunities, challenges and limitations. *Nat Rev Cancer*, 9(8):550–562, Aug 2009.

[27] Dana Faratian, Alexey Goltsov, Galina Lebedeva, Anatoly Sorokin, Stuart Moodie, Peter Mullen, Charlene Kay, In Hwa Um, Simon Langdon, Igor Goryanin, and David J Harrison. Systems biology reveals new strategies for personalizing cancer medicine and confirms the role of PTEN in resistance to trastuzumab. *Cancer Res*, 69(16):6713–6720, Aug 2009.

[28] Diane C Fingar and John Blenis. Target of rapamycin (TOR): an integrator of nutrient and growth factor signals and coordinator of cell growth and cell cycle progression. *Oncogene*, 23(18):3151–3171, Apr 2004.

[29] R. D. Fleischmann, M. D. Adams, O. White, R. A. Clayton, E. F. Kirkness, A. R. Kerlavage, C. J. Bult, J. F. Tomb, B. A. Dougherty, and J. M. Merrick. Whole-genome random sequencing and assembly of Haemophilus influenzae Rd. *Science*, 269(5223):496–512, Jul 1995.

[30] Bruno D Fonseca, Ewan M Smith, Vivian H-Y Lee, Carol MacKintosh, and Christopher G Proud. PRAS40 is a target for mammalian target of

rapamycin complex 1 and is required for signaling downstream of this complex. *J Biol Chem*, 282(34):24514–24524, Aug 2007.

[31] C.M. Fonseca, P.J. Fleming, et al. Genetic algorithms for multiobjective optimization: Formulation, discussion and generalization. In *Proceedings of the fifth international conference on genetic algorithms*, volume 423, pages 416–423. Citeseer, 1993.

[32] M. Fussenegger, J. E. Bailey, and J. Varner. A mathematical model of caspase function in apoptosis. *Nat Biotechnol*, 18(7):768–774, Jul 2000.

[33] Kapil G Gadkar, Francis J Doyle, Timothy J Crowley, and Jeffrey D Varner. Cybernetic model predictive control of a continuous bioreactor with cell recycle. *Biotechnol Prog*, 19(5):1487–1497, 2003.

[34] Attila Garami, Fried J T Zwartkruis, Takahiro Nobukuni, Manel Joaquin, Marta Roccio, Hugo Stocker, Sara C Kozma, Ernst Hafen, Johannes L Bos, and George Thomas. Insulin activation of Rheb, a mediator of mTOR/S6K/4E-BP signaling, is inhibited by TSC1 and 2. *Mol Cell*, 11(6):1457–1466, Jun 2003.

[35] A. C. Gingras, S. G. Kennedy, M. A. O'Leary, N. Sonenberg, and N. Hay. 4E-BP1, a repressor of mRNA translation, is phosphorylated and inactivated by the Akt(PKB) signaling pathway. *Genes Dev*, 12(4):502–513, Feb 1998.

[36] A. C. Gingras, B. Raught, S. P. Gygi, A. Niedzwiecka, M. Miron, S. K. Burley, R. D. Polakiewicz, A. Wyslouch-Cieszynska, R. Aebersold, and N. Sonenberg. Hierarchical phosphorylation of the translation inhibitor 4E-BP1. *Genes Dev*, 15(21):2852–2864, Nov 2001.

[37] Philippe Gual, Yannick Le Marchand-Brustel, and Jean-Franois Tanti. Positive and negative regulation of insulin signaling through IRS-1 phosphorylation. *Biochimie*, 87(1):99–109, Jan 2005.

[38] Emilie Vander Haar, Seong-Il Lee, Sricharan Bandhakavi, Timothy J Griffin, and Do-Hyung Kim. Insulin signalling to mTOR mediated by the Akt/PKB substrate PRAS40. *Nat Cell Biol*, 9(3):316–323, Mar 2007.

[39] D. Hanahan and R. A. Weinberg. The hallmarks of cancer. *Cell*, 100(1):57–70, Jan 2000.

[40] Christopher T Harbison, D. Benjamin Gordon, Tong Ihn Lee, Nicola J Rinaldi, Kenzie D Macisaac, Timothy W Danford, Nancy M Hannett, Jean-Bosco Tagne, David B Reynolds, Jane Yoo, Ezra G Jennings, Julia Zeitlinger, Dmitry K Pokholok, Manolis Kellis, P. Alex Rolfe, Ken T Takusagawa, Eric S Lander, David K Gifford, Ernest Fraenkel, and Richard A Young. Transcriptional regulatory code of a eukaryotic genome. *Nature*, 431(7004):99–104, Sep 2004.

[41] Nissim Hay and Nahum Sonenberg. Upstream and downstream of mTOR. *Genes Dev*, 18(16):1926–1945, Aug 2004.

[42] Mohamed Helmy, Jin Gohda, Jun-Ichiro Inoue, Masaru Tomita, Masa Tsuchiya, and Kumar Selvarajoo. Predicting novel features of toll-like receptor 3 signaling in macrophages. *PLoS One*, 4(3):e4661, 2009.

[43] C. Hermann, B. Assmus, C. Urbich, A. M. Zeiher, and S. Dimmeler. Insulin-mediated stimulation of protein kinase Akt: A potent survival signaling cascade for endothelial cells. *Arterioscler Thromb Vasc Biol*, 20(2):402–409, Feb 2000.

[44] A. D. HERSHEY and M. CHASE. Independent functions of viral protein and nucleic acid in growth of bacteriophage. *J Gen Physiol*, 36(1):39–56, May 1952.

[45] Marina K Holz, Bryan A Ballif, Steven P Gygi, and John Blenis. mTOR and S6K1 mediate assembly of the translation preinitiation complex through dynamic protein interchange and ordered phosphorylation events. *Cell*, 123(4):569–580, Nov 2005.

[46] Leroy Hood. Systems biology: integrating technology, biology, and computation. *Mech Ageing Dev*, 124(1):9–16, Jan 2003.

[47] Sergio Iadevaia, Yiling Lu, Fabiana C Morales, Gordon B Mills, and Prahlad T Ram. Identification of optimal drug combinations targeting cellular networks: integrating phospho-proteomics and computational network analysis. *Cancer Res*, 70(17):6704–6714, Sep 2010.

[48] Ken Inoki, Yong Li, Tianquan Zhu, Jun Wu, and Kun-Liang Guan. TSC2 is phosphorylated and inhibited by Akt and suppresses mTOR signalling. *Nat Cell Biol*, 4(9):648–657, Sep 2002.

[49] D. A. Jackson, R. H. Symons, and P. Berg. Biochemical method for inserting new genetic information into DNA of Simian Virus 40: circular SV40

DNA molecules containing lambda phage genes and the galactose operon of Escherichia coli. *Proc Natl Acad Sci U S A*, 69(10):2904–2909, Oct 1972.

[50] Richard J Jackson, Christopher U T Hellen, and Tatyana V Pestova. The mechanism of eukaryotic translation initiation and principles of its regulation. *Nat Rev Mol Cell Biol*, 11(2):113–127, Feb 2010.

[51] F. JACOB and J. MONOD. Genetic regulatory mechanisms in the synthesis of proteins. *J Mol Biol*, 3:318–356, Jun 1961.

[52] Ronald Jansen, Haiyuan Yu, Dov Greenbaum, Yuval Kluger, Nevan J Krogan, Sambath Chung, Andrew Emili, Michael Snyder, Jack F Greenblatt, and Mark Gerstein. A Bayesian networks approach for predicting protein-protein interactions from genomic data. *Science*, 302(5644):449–453, Oct 2003.

[53] H. Jiang and P. K. Vogt. Constitutively active Rheb induces oncogenic transformation. *Oncogene*, 27(43):5729–5740, Sep 2008.

[54] I. S. Johnson. Human insulin from recombinant DNA technology. *Science*, 219(4585):632–637, Feb 1983.

[55] Andrew R Joyce and Bernhard Palsson. The model organism as a system: integrating 'omics' data sets. *Nat Rev Mol Cell Biol*, 7(3):198–210, Mar 2006.

[56] Tae Hoon Kim, Leah O Barrera, Ming Zheng, Chunxu Qu, Michael A Singer, Todd A Richmond, Yingnian Wu, Roland D Green, and Bing Ren. A high-resolution map of active promoters in the human genome. *Nature*, 436(7052):876–880, Aug 2005.

[57] Marc W Kirschner. The meaning of systems biology. *Cell*, 121(4):503–504, May 2005.

[58] Hiroaki Kitano. Computational systems biology. *Nature*, 420(6912):206–210, Nov 2002.

[59] Hiroaki Kitano. Systems biology: a brief overview. *Science*, 295(5560):1662–1664, Mar 2002.

[60] R. Kohavi. A study of cross-validation and bootstrap for accuracy estimation and model selection. In *International joint Conference on artificial intelligence*, volume 14, pages 1137–1145. Citeseer, 1995.

[61] Esther Latres, Ami R Amini, Ashley A Amini, Jennifer Griffiths, Francis J Martin, Yi Wei, Hsin Chieh Lin, George D Yancopoulos, and David J Glass. Insulin-like growth factor-1 (IGF-1) inversely regulates atrophy-induced genes via the phosphatidylinositol 3-kinase/Akt/mammalian target of rapamycin (PI3K/Akt/mTOR) pathway. *J Biol Chem*, 280(4):2737–2744, Jan 2005.

[62] J. Li, K. DeFea, and R. A. Roth. Modulation of insulin receptor substrate-1 tyrosine phosphorylation by an Akt/phosphatidylinositol 3-kinase pathway. *J Biol Chem*, 274(14):9351–9356, Apr 1999.

[63] M. N. Lioubin, P. A. Algate, S. Tsai, K. Carlberg, A. Aebersold, and L. R. Rohrschneider. p150Ship, a signal transduction molecule with inositol polyphosphate-5-phosphatase activity. *Genes Dev*, 10(9):1084–1095, May 1996.

[64] Hong Liu, Derek C Radisky, Celeste M Nelson, Hui Zhang, Jimmie E Fata, Richard A Roth, and Mina J Bissell. Mechanism of Akt1 inhibition of breast cancer cell invasion reveals a protumorigenic role for TSC2. *Proc Natl Acad Sci U S A*, 103(11):4134–4139, Mar 2006.

[65] P. E. Lobban and A. D. Kaiser. Enzymatic end-to end joining of DNA molecules. *J Mol Biol*, 78(3):453–471@inproceedingsfonseca1993genetic, title=Genetic algorithms for multiobjective optimization: Formulation, discussion and generalization, author=Fonseca, C.M. and Fleming, P.J. and others, booktitle=Proceedings of the fifth international conference on genetic algorithms, volume=423, pages=416–423, year=1993, organization=Citeseer , Aug 1973.

[66] J. R. Lorsch and D. Herschlag. Kinetic dissection of fundamental processes of eukaryotic translation initiation in vitro. *EMBO J*, 18(23):6705–6717, Dec 1999.

[67] Xiaoju Max Ma and John Blenis. Molecular mechanisms of mTOR-mediated translational control. *Nat Rev Mol Cell Biol*, 10(5):307–318, May 2009.

[68] Xiaoju Max Ma, Sang-Oh Yoon, Celeste J Richardson, Kristina Julich, and John Blenis. SKAR links pre-mRNA splicing to mTOR/S6K1-mediated enhanced translation efficiency of spliced mRNAs. *Cell*, 133(2):303–313, Apr 2008.

[69] Colin Macilwain. Systems biology: evolving into the mainstream. *Cell*, 144(6):839–841, Mar 2011.

[70] Brendan D Manning, Andrew R Tee, M. Nicole Logsdon, John Blenis, and Lewis C Cantley. Identification of the tuberous sclerosis complex-2 tumor suppressor gene product tuberin as a target of the phosphoinositide 3-kinase/akt pathway. *Mol Cell*, 10(1):151–162, Jul 2002.

[71] Assen Marintchev and Gerhard Wagner. Translation initiation: structures, mechanisms and evolution. *Q Rev Biophys*, 37(3-4):197–284, 2004.

[72] Alfonso Mora, David Komander, Daan M F van Aalten, and Dario R Alessi. PDK1, the master regulator of AGC kinase signal transduction. *Semin Cell Dev Biol*, 15(2):161–170, Apr 2004.

[73] Katsutaro Morino, Kitt Falk Petersen, and Gerald I Shulman. Molecular mechanisms of insulin resistance in humans and their potential links with mitochondrial dysfunction. *Diabetes*, 55 Suppl 2:S9–S15, Dec 2006.

[74] M. G. Myers, R. Mendez, P. Shi, J. H. Pierce, R. Rhoads, and M. F. White. The COOH-terminal tyrosine phosphorylation sites on IRS-1 bind SHP-2 and negatively regulate insulin signaling. *J Biol Chem*, 273(41):26908–26914, Oct 1998.

[75] S. Nayak, J. K. Siddiqui, and J. D. Varner. Modelling and analysis of an ensemble of eukaryotic translation initiation models. *IET Systems Biology*, 5(1):2–14, 2011.

[76] Satyaprakash Nayak, Saniya Salim, Deyan Luan, Michael Zai, and Jeffrey D Varner. A test of highly optimized tolerance reveals fragile cell-cycle mechanisms are molecular targets in clinical cancer trials. *PLoS One*, 3(4):e2016, 2008.

[77] Scott D Patterson and Ruedi H Aebersold. Proteomics: the first decade and beyond. *Nat Genet*, 33 Suppl:311–323, Mar 2003.

[78] K. Paz, R. Hemi, D. LeRoith, A. Karasik, E. Elhanany, H. Kanety, and Y. Zick. A molecular basis for insulin resistance. Elevated serine/threonine phosphorylation of IRS-1 and IRS-2 inhibits their binding to the juxtamembrane region of the insulin receptor and impairs their ability to undergo insulin-induced tyrosine phosphorylation. *J Biol Chem*, 272(47):29911–29918, Nov 1997.

[79] K. Paz, Y. F. Liu, H. Shorer, R. Hemi, D. LeRoith, M. Quan, H. Kanety, R. Seger, and Y. Zick. Phosphorylation of insulin receptor substrate-1 (IRS-1) by protein kinase B positively regulates IRS-1 function. *J Biol Chem*, 274(40):28816–28822, Oct 1999.

[80] Nathan D Price, Jennifer L Reed, and Bernhard Palsson. Genome-scale models of microbial cells: evaluating the consequences of constraints. *Nat Rev Microbiol*, 2(11):886–897, Nov 2004.

[81] B. Raught, A. C. Gingras, S. P. Gygi, H. Imataka, S. Morino, A. Gradi, R. Aebersold, and N. Sonenberg. Serum-stimulated, rapamycin-sensitive phosphorylation sites in the eukaryotic translation initiation factor 4GI. *EMBO J*, 19(3):434–444, Feb 2000.

[82] Brian Raught, Franck Peiretti, Anne-Claude Gingras, Mark Livingstone, David Shahbazian, Greg L Mayeur, Roberto D Polakiewicz, Nahum Sonenberg, and John W B Hershey. Phosphorylation of eucaryotic translation initiation factor 4B Ser422 is modulated by S6 kinases. *EMBO J*, 23(8):1761–1769, Apr 2004.

[83] Jennifer L Reed, Iman Famili, Ines Thiele, and Bernhard O Palsson. Towards multidimensional genome annotation. *Nat Rev Genet*, 7(2):130–141, Feb 2006.

[84] Daniel R Rhodes, Scott A Tomlins, Sooryanarayana Varambally, Vasudeva Mahavisno, Terrence Barrette, Shanker Kalyana-Sundaram, Debashis Ghosh, Akhilesh Pandey, and Arul M Chinnaiyan. Probabilistic model of the human protein-protein interaction network. *Nat Biotechnol*, 23(8):951–959, Aug 2005.

[85] J. M. Ricort, J. F. Tanti, E. Van Obberghen, and Y. Le Marchand-Brustel. Cross-talk between the platelet-derived growth factor and the insulin signaling pathways in 3T3-L1 adipocytes. *J Biol Chem*, 272(32):19814–19818, Aug 1997.

[86] Richard J Roberts. How restriction enzymes became the workhorses of molecular biology. *Proc Natl Acad Sci U S A*, 102(17):5905–5908, Apr 2005.

[87] P. Rodriguez-Viciana, P. H. Warne, R. Dhand, B. Vanhaesebroeck, I. Gout, M. J. Fry, M. D. Waterfield, and J. Downward. Phosphatidylinositol-3-OH kinase as a direct target of Ras. *Nature*, 370(6490):527–532, Aug 1994.

[88] Deepali Sachdev and Douglas Yee. Disrupting insulin-like growth factor signaling as a potential cancer therapy. *Mol Cancer Ther*, 6(1):1–12, Jan 2007.

[89] M.G. Safonov. *Stability and robustness of multivariable feedback systems*. MIT Press, 1980.

[90] Leonardo Salmena, Arkaitz Carracedo, and Pier Paolo Pandolfi. Tenets of PTEN tumor suppression. *Cell*, 133(3):403–414, May 2008.

[91] A. R. Saltiel and C. R. Kahn. Insulin signalling and the regulation of glucose and lipid metabolism. *Nature*, 414(6865):799–806, Dec 2001.

[92] Alan R Saltiel and Jeffrey E Pessin. Insulin signaling pathways in time and space. *Trends Cell Biol*, 12(2):65–71, Feb 2002.

[93] Yardena Samuels, Zhenghe Wang, Alberto Bardelli, Natalie Silliman, Janine Ptak, Steve Szabo, Hai Yan, Adi Gazdar, Steven M Powell, Gregory J Riggins, James K V Willson, Sanford Markowitz, Kenneth W Kinzler, Bert Vogelstein, and Victor E Velculescu. High frequency of mutations of the PIK3CA gene in human cancers. *Science*, 304(5670):554, Apr 2004.

[94] Yasemin Sancak, Carson C Thoreen, Timothy R Peterson, Robert A Lindquist, Seong A Kang, Eric Spooner, Steven A Carr, and David M Sabatini. PRAS40 is an insulin-regulated inhibitor of the mTORC1 protein kinase. *Mol Cell*, 25(6):903–915, Mar 2007.

[95] F. Sanger, S. Nicklen, and A. R. Coulson. DNA sequencing with chain-terminating inhibitors. *Proc Natl Acad Sci U S A*, 74(12):5463–5467, Dec 1977.

[96] D. D. Sarbassov, David A Guertin, Siraj M Ali, and David M Sabatini. Phosphorylation and regulation of Akt/PKB by the rictor-mTOR complex. *Science*, 307(5712):1098–1101, Feb 2005.

[97] Satoru Sasagawa, Yu ichi Ozaki, Kazuhiro Fujita, and Shinya Kuroda. Prediction and validation of the distinct dynamics of transient and sustained ERK activation. *Nat Cell Biol*, 7(4):365–373, Apr 2005.

[98] Leslie J Saucedo, Xinsheng Gao, Dominic A Chiarelli, Ling Li, Duoija Pan, and Bruce A Edgar. Rheb promotes cell growth as a component of the insulin/TOR signalling network. *Nat Cell Biol*, 5(6):566–571, Jun 2003.

[99] M. Schena, D. Shalon, R. W. Davis, and P. O. Brown. Quantitative monitoring of gene expression patterns with a complementary DNA microarray. *Science*, 270(5235):467–470, Oct 1995.

[100] Gert C Scheper and Christopher G Proud. Does phosphorylation of the cap-binding protein eIF4E play a role in translation initiation? *Eur J Biochem*, 269(22):5350–5359, Nov 2002.

[101] R.J. Schneider, N. Sonenberg, M. Mathews, N. Sonenberg, and J. Hershey. Translational control in cancer development and progression. *Translational control in biology and medicine*, pages 401–431, 2007.

[102] Birgit Schoeberl, Claudia Eichler-Jonsson, Ernst Dieter Gilles, and Gertraud Mller. Computational modeling of the dynamics of the MAP kinase cascade activated by surface and internalized EGF receptors. *Nat Biotechnol*, 20(4):370–375, Apr 2002.

[103] E Schrodinger. *What is Life?* Cambridge Univ Press, 1944.

[104] E. Y. Skolnik, A. Batzer, N. Li, C. H. Lee, E. Lowenstein, M. Mohammadi, B. Margolis, and J. Schlessinger. The function of GRB2 in linking the insulin receptor to Ras signaling pathways. *Science*, 260(5116):1953–1955, Jun 1993.

[105] E. Y. Skolnik, C. H. Lee, A. Batzer, L. M. Vicentini, M. Zhou, R. Daly, M. J. Myers, J. M. Backer, A. Ullrich, and M. F. White. The SH2/SH3 domain-containing protein GRB2 interacts with tyrosine-phosphorylated IRS1 and Shc: implications for insulin control of ras signalling. *EMBO J*, 12(5):1929–1936, May 1993.

[106] H. O. Smith and K. W. Wilcox. A restriction enzyme from Hemophilus influenzae. I. Purification and general properties. *J Mol Biol*, 51(2):379–391, Jul 1970.

[107] Sang Ok Song, Anirikh Chakrabarti, and Jeffrey D Varner. Ensembles of signal transduction models using Pareto Optimal Ensemble Techniques (POETs). *Biotechnol J*, 5(7):768–780, Jul 2010.

[108] Sang Ok Song and Jeffrey Varner. Modeling and analysis of the molecular basis of pain in sensory neurons. *PLoS One*, 4(9):e6758, 2009.

[109] Jrg Stelling, Ernst Dieter Gilles, and Francis J Doyle. Robustness

properties of circadian clock architectures. *Proc Natl Acad Sci U S A*, 101(36):13210–13215, Sep 2004.

[110] Jrg Stelling, Uwe Sauer, Zoltan Szallasi, Francis J Doyle, and John Doyle. Robustness of cellular functions. *Cell*, 118(6):675–685, Sep 2004.

[111] Ulrich Stelzl, Uwe Worm, Maciej Lalowski, Christian Haenig, Felix H Brembeck, Heike Goehler, Martin Stroedicke, Martina Zenkner, Anke Schoenherr, Susanne Koeppen, Jan Timm, Sascha Mintzlaff, Claudia Abraham, Nicole Bock, Silvia Kietzmann, Astrid Goedde, Engin Toksz, Anja Droege, Sylvia Krobitsch, Bernhard Korn, Walter Birchmeier, Hans Lehrach, and Erich E Wanker. A human protein-protein interaction network: a resource for annotating the proteome. *Cell*, 122(6):957–968, Sep 2005.

[112] E. C. Strauss, J. A. Kobori, G. Siu, and L. E. Hood. Specific-primer-directed DNA sequencing. *Anal Biochem*, 154(1):353–360, Apr 1986.

[113] H. Sun, R. Lesche, D. M. Li, J. Liliental, H. Zhang, J. Gao, N. Gavrilova, B. Mueller, X. Liu, and H. Wu. PTEN modulates cell cycle progression and cell survival by regulating phosphatidylinositol 3,4,5,-trisphosphate and Akt/protein kinase B signaling pathway. *Proc Natl Acad Sci U S A*, 96(11):6199–6204, May 1999.

[114] Yoko Takahashi, Fabiana C Morales, Erica L Kreimann, and Maria-Magdalena Georgescu. PTEN tumor suppressor associates with NHERF proteins to attenuate PDGF receptor signaling. *EMBO J*, 25(4):910–920, Feb 2006.

[115] Amos Tanay, Roded Sharan, Martin Kupiec, and Ron Shamir. Revealing modularity and organization in the yeast molecular network by integrated analysis of highly heterogeneous genomewide data. *Proc Natl Acad Sci U S A*, 101(9):2981–2986, Mar 2004.

[116] Cullen M Taniguchi, Brice Emanuelli, and C. Ronald Kahn. Critical nodes in signalling pathways: insights into insulin action. *Nat Rev Mol Cell Biol*, 7(2):85–96, Feb 2006.

[117] Ryan Tasseff, Satyaprakash Nayak, Saniya Salim, Poorvi Kaushik, Noreen Rizvi, and Jeffrey D Varner. Analysis of the molecular networks in androgen dependent and independent prostate cancer revealed fragile and robust subsystems. *PLoS One*, 5(1):e8864, 2010.

[118] Ryan Tasseff, Satyaprakash Nayak, Sang Ok Song, Andrew Yen, and Jeffrey D Varner. Modeling and analysis of retinoic acid induced differentiation of uncommitted precursor cells. *Integr Biol (Camb)*, 3(5):578–591, May 2011.

[119] Alexandros Tzatsos and Konstantin V Kandror. Nutrients suppress phosphatidylinositol 3-kinase/Akt signaling via raptor-dependent mTOR-mediated insulin receptor substrate 1 phosphorylation. *Mol Cell Biol*, 26(1):63–76, Jan 2006.

[120] Kohjiro Ueki, Tatsuya Kondo, and C. Ronald Kahn. Suppressor of cytokine signaling 1 (SOCS-1) and SOCS-3 cause insulin resistance through inhibition of tyrosine phosphorylation of insulin receptor substrate proteins by discrete mechanisms. *Mol Cell Biol*, 24(12):5434–5446, Jun 2004.

[121] Sung Hee Um, David D'Alessio, and George Thomas. Nutrient overload, insulin resistance, and ribosomal protein S6 kinase 1, S6K1. *Cell Metab*, 3(6):393–402, Jun 2006.

[122] Sung Hee Um, Francesca Frigerio, Mitsuhiro Watanabe, Frdric Picard, Manel Joaquin, Melanie Sticker, Stefano Fumagalli, Peter R Allegrini, Sara C Kozma, Johan Auwerx, and George Thomas. Absence of S6K1 protects against age- and diet-induced obesity while enhancing insulin sensitivity. *Nature*, 431(7005):200–205, Sep 2004.

[123] J. D. Varner. Large-scale prediction of phenotype: concept. *Biotechnol Bioeng*, 69(6):664–678, Sep 2000.

[124] J. C. Venter, M. D. Adams, E. W. Myers, P. W. Li, R. J. Mural, G. G. Sutton, H. O. Smith, M. Yandell, C. A. Evans, R. A. Holt, J. D. Gocayne, P. Amanatides, R. M. Ballew, D. H. Huson, J. R. Wortman, Q. Zhang, C. D. Kodira, X. H. Zheng, L. Chen, M. Skupski, G. Subramanian, P. D. Thomas, J. Zhang, G. L. Gabor Miklos, C. Nelson, S. Broder, A. G. Clark, J. Nadeau, V. A. McKusick, N. Zinder, A. J. Levine, R. J. Roberts, M. Simon, C. Slayman, M. Hunkapiller, R. Bolanos, A. Delcher, I. Dew, D. Fasulo, M. Flanigan, L. Florea, A. Halpern, S. Hannenhalli, S. Kravitz, S. Levy, C. Mobarry, K. Reinert, K. Remington, J. Abu-Threideh, E. Beasley, K. Biddick, V. Bonazzi, R. Brandon, M. Cargill, I. Chandramouliswaran, R. Charlab, K. Chaturvedi, Z. Deng, V. Di Francesco, P. Dunn, K. Eilbeck, C. Evangelista, A. E. Gabrielian, W. Gan, W. Ge, F. Gong, Z. Gu, P. Guan, T. J. Heiman, M. E. Higgins, R. R. Ji, Z. Ke, K. A. Ketchum, Z. Lai, Y. Lei, Z. Li, J. Li, Y. Liang, X. Lin, F. Lu, G. V. Merkulov, N. Milshina, H. M. Moore, A. K. Naik, V. A. Narayan, B. Neelam, D. Nusskern, D. B. Rusch,

S. Salzberg, W. Shao, B. Shue, J. Sun, Z. Wang, A. Wang, X. Wang, J. Wang, M. Wei, R. Wides, C. Xiao, C. Yan, A. Yao, J. Ye, M. Zhan, W. Zhang, H. Zhang, Q. Zhao, L. Zheng, F. Zhong, W. Zhong, S. Zhu, S. Zhao, D. Gilbert, S. Baumhueter, G. Spier, C. Carter, A. Cravchik, T. Woodage, F. Ali, H. An, A. Awe, D. Baldwin, H. Baden, M. Barnstead, I. Barrow, K. Beeson, D. Busam, A. Carver, A. Center, M. L. Cheng, L. Curry, S. Danaher, L. Davenport, R. Desilets, S. Dietz, K. Dodson, L. Doup, S. Ferriera, N. Garg, A. Gluecksmann, B. Hart, J. Haynes, C. Haynes, C. Heiner, S. Hladun, D. Hostin, J. Houck, T. Howland, C. Ibegwam, J. Johnson, F. Kalush, L. Kline, S. Koduru, A. Love, F. Mann, D. May, S. McCawley, T. McIntosh, I. McMullen, M. Moy, L. Moy, B. Murphy, K. Nelson, C. Pfannkoch, E. Pratts, V. Puri, H. Qureshi, M. Reardon, R. Rodriguez, Y. H. Rogers, D. Romblad, B. Ruhfel, R. Scott, C. Sitter, M. Smallwood, E. Stewart, R. Strong, E. Suh, R. Thomas, N. N. Tint, S. Tse, C. Vech, G. Wang, J. Wetter, S. Williams, M. Williams, S. Windsor, E. Winn-Deen, K. Wolfe, J. Zaveri, K. Zaveri, J. F. Abril, R. Guig, M. J. Campbell, K. V. Sjolander, B. Karlak, A. Kejariwal, H. Mi, B. Lazareva, T. Hatton, A. Narechania, K. Diemer, A. Muruganujan, N. Guo, S. Sato, V. Bafna, S. Istrail, R. Lippert, R. Schwartz, B. Walenz, S. Yooseph, D. Allen, A. Basu, J. Baxendale, L. Blick, M. Caminha, J. Carnes-Stine, P. Caulk, Y. H. Chiang, M. Coyne, C. Dahlke, A. Mays, M. Dombroski, M. Donnelly, D. Ely, S. Esparham, C. Fosler, H. Gire, S. Glanowski, K. Glasser, A. Glodek, M. Gorokhov, K. Graham, B. Gropman, M. Harris, J. Heil, S. Henderson, J. Hoover, D. Jennings, C. Jordan, J. Jordan, J. Kasha, L. Kagan, C. Kraft, A. Levitsky, M. Lewis, X. Liu, J. Lopez, D. Ma, W. Majoros, J. McDaniel, S. Murphy, M. Newman, T. Nguyen, N. Nguyen, M. Nodell, S. Pan, J. Peck, M. Peterson, W. Rowe, R. Sanders, J. Scott, M. Simpson, T. Smith, A. Sprague, T. Stockwell, R. Turner, E. Venter, M. Wang, M. Wen, D. Wu, M. Wu, A. Xia, A. Zandieh, and X. Zhu. The sequence of the human genome. *Science*, 291(5507):1304–1351, Feb 2001.

[125] Priam Villalonga, Silvia Fernndez de Mattos, and Anne J Ridley. RhoE inhibits 4E-BP1 phosphorylation and eIF4E function impairing cap-dependent translation. *J Biol Chem*, 284(51):35287–35296, Dec 2009.

[126] R. G. Vries, A. Flynn, J. C. Patel, X. Wang, R. M. Denton, and C. G. Proud. Heat shock increases the association of binding protein-1 with initiation factor 4E. *J Biol Chem*, 272(52):32779–32784, Dec 1997.

[127] Lifu Wang, Thurl E Harris, and John C Lawrence. Regulation of proline-rich Akt substrate of 40 kDa (PRAS40) function by mammalian target of rapamycin complex 1 (mTORC1)-mediated phosphorylation. *J Biol Chem*, 283(23):15619–15627, Jun 2008.

[128] J. D. WATSON and F. H. CRICK. Molecular structure of nucleic acids; a structure for deoxyribose nucleic acid. *Nature*, 171(4356):737–738, Apr 1953.

[129] Timothy A Yap, Michelle D Garrett, Mike I Walton, Florence Raynaud, Johann S de Bono, and Paul Workman. Targeting the PI3K-AKT-mTOR pathway: progress, pitfalls, and promises. *Curr Opin Pharmacol*, 8(4):393–412, Aug 2008.

[130] Esti Yeger-Lotem, Shmuel Sattath, Nadav Kashtan, Shalev Itzkovitz, Ron Milo, Ron Y Pinter, Uri Alon, and Hanah Margalit. Network motifs in integrated cellular networks of transcription-regulation and protein-protein interaction. *Proc Natl Acad Sci U S A*, 101(16):5934–5939, Apr 2004.

[131] T. L. Yuan and L. C. Cantley. PI3K pathway alterations in cancer: variations on a theme. *Oncogene*, 27(41):5497–5510, Sep 2008.

[132] S. G. Zimmer, A. DeBenedetti, and J. R. Graff. Translational control of malignancy: the mRNA cap-binding protein, eIF-4E, as a central regulator of tumor formation, growth, invasion and metastasis. *Anticancer Res*, 20(3A):1343–1351, 2000.

[133] Roberto Zoncu, Alejo Efeyan, and David M Sabatini. mTOR: from growth signal integration to cancer, diabetes and ageing. *Nat Rev Mol Cell Biol*, 12(1):21–35, Jan 2011.